iScience

CellPress
OPEN ACCESS

Article

Tomatidine targets ATF4-dependent signaling and induces ferroptosis to limit pancreatic cancer progression

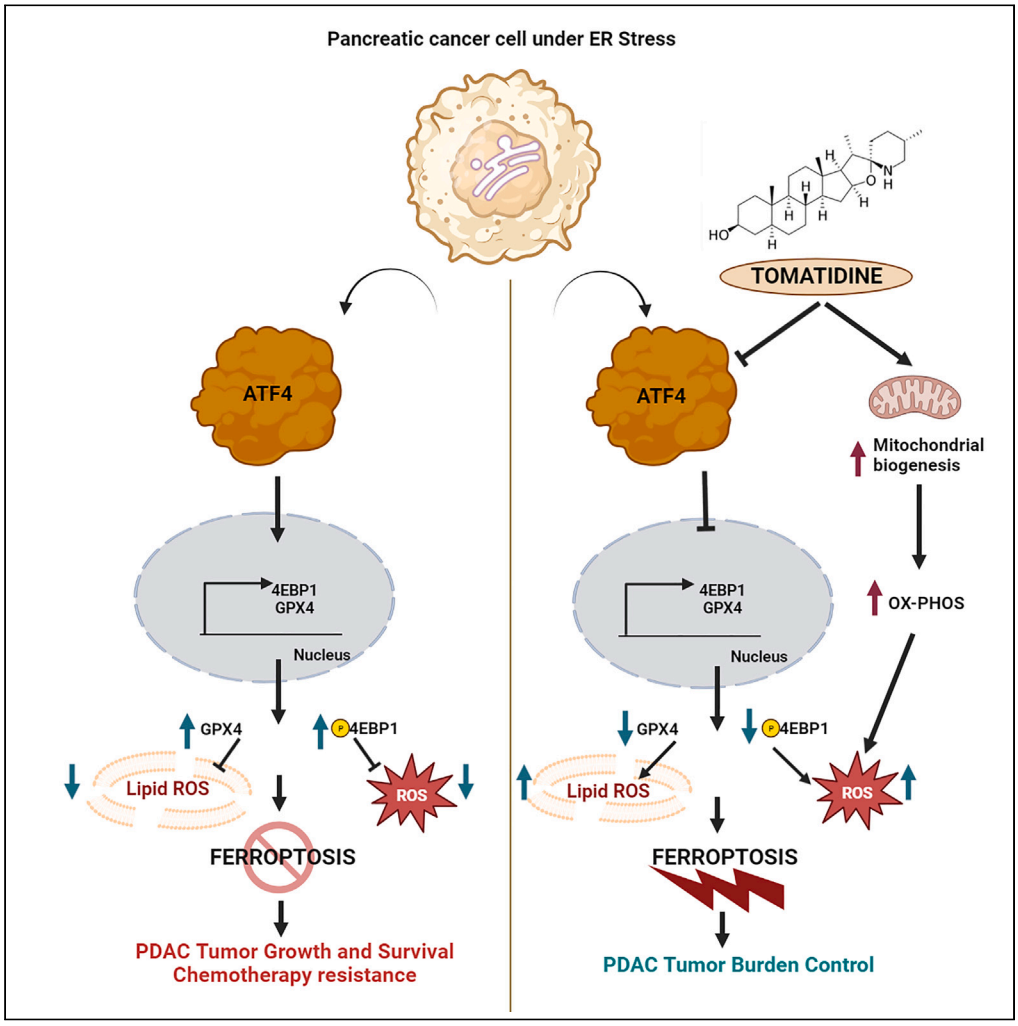

Debasmita Mukherjee, Srija Chakraborty, Lena Bercz, ..., Anne M. Strohecker, Aleksander Skardal, Thomas A. Mace

Thomas.Mace@osumc.edu

Highlights

ATF4, a transcription factor regulating stress, is a target in pancreatic cancer

Tomatidine inhibits pancreatic tumor growth and enhances gemcitabine chemosensitivity

Tomatidine reduces binding of ATF4 with downstream promoter elements

Tomatidine induces ferroptosis-mediated cell death in pancreatic cancer cells

Mukherjee et al., iScience 26, 107408
August 18, 2023
https://doi.org/10.1016/j.isci.2023.107408

iScience

CellPress
OPEN ACCESS

Article

Tomatidine targets ATF4-dependent signaling and induces ferroptosis to limit pancreatic cancer progression

Debasmita Mukherjee,[1,2] Srija Chakraborty,[1,3] Lena Bercz,[1] Liliana D'Alesio,[1] Jessica Wedig,[1,2] Molly A. Torok,[1] Timothy Pfau,[1] Hannah Lathrop,[1] Shrina Jasani,[1] Abigail Guenther,[1] Jake McGue,[4] Daniel Adu-Ampratwum,[5] James R. Fuchs,[5] Timothy L. Frankel,[4] Maciej Pietrzak,[6] Stacey Culp,[6] Anne M. Strohecker,[1,7] Aleksander Skardal,[1,3] and Thomas A. Mace[1,8,9,10,*]

SUMMARY

Pancreatic ductal adenocarcinoma (PDAC) is an aggressive cancer with high metastasis and therapeutic resistance. Activating transcription factor 4 (ATF4), a master regulator of cellular stress, is exploited by cancer cells to survive. Prior research and data reported provide evidence that high ATF4 expression correlates with worse overall survival in PDAC. Tomatidine, a natural steroidal alkaloid, is associated with inhibition of ATF4 signaling in multiple diseases. Here, we discovered that *in vitro* and *in vivo* tomatidine treatment of PDAC cells inhibits tumor growth. Tomatidine inhibited nuclear translocation of ATF4 and reduced the transcriptional binding of ATF4 with downstream promoters. Tomatidine enhanced gemcitabine chemosensitivity in 3D ECM-hydrogels and *in vivo*. Tomatidine treatment was associated with induction of ferroptosis signaling validated by increased lipid peroxidation, mitochondrial biogenesis, and decreased GPX4 expression in PDAC cells. This study highlights a possible therapeutic approach utilizing a plant-derived metabolite, tomatidine, to target ATF4 activity in PDAC.

INTRODUCTION

Pancreatic cancer is very aggressive and has a dismal five-year survival rate of 12%.[1] Pancreatic ductal adenocarcinoma (PDAC), the cancer that develops from the exocrine cells of the pancreas and represents ~90% of pancreatic cancer cases, is usually diagnosed in advanced stages and has a poor prognosis as compared to other pancreatic cancers. One of the only curative therapies available is neoadjuvant chemotherapy followed by surgical resection. However, only 10%–20% of patients are eligible for surgery while most of the residual 80%–90% of patients show non-resectable disease with distant metastases. Systemic chemotherapy encompassing nucleoside analogs such as gemcitabine or 5-fluorouracil in combination with radiotherapy or other treatment modalities such as administration of albumin nanoparticles-bound paclitaxel (nab-paclitaxel) are standard-of-care therapies for non-resectable disease. Unfortunately, these treatment modalities are often met with issues of cellular toxicity and therapeutic resistance.[2,3]

Activating transcription factor 4 (ATF4), a basic region-leucine zipper transcription factor, functions as a master regulator of stress response.[4] ATF4 can also act as a developmental regulator binding to C/EBP-ATF response elements in the promoter regions of target genes and can activate transcription of downstream genes.[4] ATF4 participates in the unfolded protein response as well as the integrated stress response (ISR).[5] ATF4 can switch between activation of pro-survival and pro-apoptotic genes that induce the expression of downstream proteins such as 4EBP1[6,7] or C/EBP homologous protein (CHOP), respectively, in normal cells.[8,9] Further, ATF4 along with CHOP can dephosphorylate eIF2α and generate reactive oxygen species (ROS) by regulating the gene expression of different redox enzymes. These processes lead to generation of ROS with an increased nascent protein load.[10] However, cancer cells can exploit ATF4-dependent signaling and transcription machinery to help them survive, persist, and resist therapeutics in stressful and nutrient-deprived microenvironments. ATF4 overexpression has also been elucidated as one of the causes of gemcitabine chemoresistance in PDAC.[11–14]

[1]The James Comprehensive Cancer Center, Ohio State University Wexner Medical Center, Columbus, OH 43210, USA

[2]Molecular, Cellular and Developmental Biology Program, The Ohio State University, Columbus, OH 43210, USA

[3]Department of Biomedical Engineering, The Ohio State University, Columbus, OH 43210, USA

[4]Department of Surgery, University of Michigan, Ann Arbor, MI 48109, USA

[5]Division of Medicinal Chemistry & Pharmacognosy, The Ohio State University, Columbus, OH 43210, USA

[6]Department of Biomedical Informatics, The Ohio State University, Columbus, OH 43210, USA

[7]Department of Cancer Biology & Genetics, The Ohio State University, Columbus, OH 43210, USA

[8]Department of Internal Medicine, Division of Gastroenterology, Hepatology, and Nutrition, The Ohio State University, Columbus, OH 43210, USA

[9]Twitter: TMaceLab

[10]Lead contact

*Correspondence: Thomas.Mace@osumc.edu

https://doi.org/10.1016/j.isci.2023.107408

Anticancer agents can cause cancer cell death generally through established mechanisms of death such as caspase-dependent pathways like apoptosis. However, there are non-caspase-dependent mechanisms of cancer cell death such as necroptosis, pyroptosis, and ferroptosis.[15] Increased iron accumulation in cells can cause ferroptosis-mediated programmed cell death leading to accumulation of ROS and lipid peroxidation.[16] Targeting the cell death process is becoming more and more common in cancer treatment, especially to tackle issues of therapy resistance. Cancer cells have been reported to significantly enhance their oxidative stress defense by inhibiting ferroptosis and increasing resistant survival.[17,18] Many studies have shown ferroptosis in cancer cells is sufficient to overcome resistance to traditional chemotherapy, targeted therapy, and immunotherapy.[19] ATF4 induction via ER stress can enable cancer cell survival and acquired drug resistance by inhibiting ferroptosis.[9,20,21]

Numerous studies have indicated that natural products obtained from plant sources such as paclitaxel, vinblastine, vincristine, irinotecan, and topotecan exert selective toxicity toward cancer cells and can act as lead compounds for synthesis of derivatives/synthetic molecules that function as active pharmacophores.[22,23] Complex dietary foods such as tomatoes are often composed of metabolites that have anti-inflammatory and chemopreventive properties. One such naturally occurring metabolite present in tomatoes is a steroidal alkaloid and aglycone product metabolized from α-tomatine known as tomatidine. α-Tomatine and tomatidine are mainly present in the skin of unripe green tomatoes and sometimes in the tomato leaves and flowers.[24] Tomatidine is comparatively less cytotoxic than α-tomatine and has been tested *in vivo*.[24–26] Tomatidine has been shown to be a potent and effective chemosensitizer in multidrug-resistant tumor cells and can inhibit tumor cell proliferation and invasion in lung, liver, and colon cancer cell lines.[27–29] Further, tomatidine was bioinformatically identified as one of the candidate agents to work as a drug against pancreatic cancer.[30] Although there is evidence of tomatidine being systemically detectable after consumption of tomatoes, there is little understanding pertaining to its effects on the growth of cancer cells. Investigators have shown that tomatidine may target skeletal muscle ATF4 expression leading to reductions in age-related deficits in skeletal muscle strength, quality, and mass. This study elucidates ATF4 as a critical mediator of age-related muscle weakness and atrophy and identifies tomatidine as a potential agent and/or lead compound for reducing ATF4 activity, weakness, and atrophy in aged skeletal muscle.[31,32] However, direct evidence of tomatidine affecting ATF4 activity and its downstream signaling has not been shown, especially in the context of cancer.

In this study, we hypothesized that tomatidine can limit pancreatic cancer by regulating ATF4-dependent signaling. We observed that tomatidine inhibits pancreatic tumor growth *in vitro* and *in vivo*. Tomatidine also enhanced the gemcitabine chemosensitivity in an orthotopic model of pancreatic cancer *in vivo*. Tomatidine reduced phosphorylation of 4EBP1 (downstream of ATF4) *in vitro* and reduced mRNA expression of ATF4 and eIF4EBP1 in tumor-bearing mice treated with tomatidine. Tomatidine limited nuclear translocation of ATF4 and reduced the transcriptional binding activity of ATF4 with downstream genes. Further, we found that tomatidine is a novel inducer of ferroptosis-mediated cell death. Overall, this study investigates a plant-derived anticancer treatment as a novel therapeutic approach against pancreatic cancer and its tumor microenvironment.

RESULTS

Tomatidine inhibits pancreatic tumor growth *in vitro*

To determine whether tomatidine inhibits the proliferation of human pancreatic cancer cells, we used human (MiaPaca-2, Panc1) as well as murine (MT5) pancreatic cancer cells. These cell lines were tested for viability using an MTT assay after incubation with doses ranging from 0 to 12.8 μg/mL of tomatidine for 3 days. Tomatidine inhibited the proliferation of all the pancreatic cancer cell lines in a dose-dependent manner (Figures 1A–1C). We next tested whether tomatidine can induce apoptosis in MiaPaca-2 (Figure 1D), Panc1 (Figure 1E), and MT5 (Figure 1F) using Annexin V/PI assay. Our results showed that tomatidine can increase cell death in a dose-dependent manner.

RNA sequencing reveals that tomatidine modulates ATF4-dependent ER stress genes in pancreatic cancer cells

To understand how tomatidine affects the pancreatic cancer cells, we compared the global transcriptome of untreated vs. tomatidine-treated Panc1 and MT5 cells by RNA sequencing. We treated the Panc1 and MT5 cells with/without 6.4 μg/mL tomatidine for 40 h. Differential expression analysis between tomatidine-treated human pancreatic cancer cell line (Panc1) samples and controls revealed that 865 genes

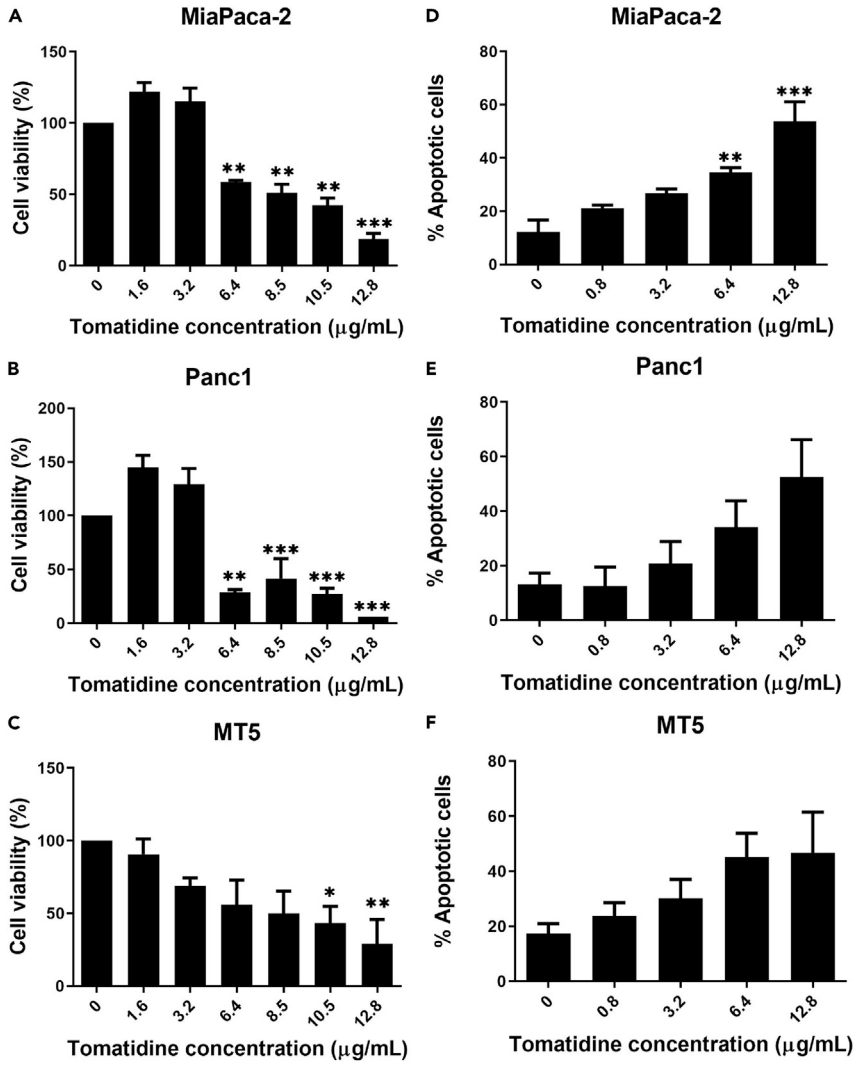

Figure 1. Tomatidine inhibits pancreatic tumor growth *in vitro*

(A–C) (A) MiaPaca-2, (B) Panc1 (human), and (C) MT5 (murine) pancreatic tumor cell lines were treated with increasing concentrations of tomatidine for 72 h and assayed for cell growth via MTT assay.

(D–F) (D) MiaPaca-2, (E) Panc1, and (F) MT5 were treated with increasing concentrations of tomatidine for 72 h and assayed for cell death via Annexin V/PI assay. Data are reported as the means + SEMs. n = 3 or more independent biological replicates (One-way ANOVA with Tukey's test for pairwise comparisons was used to analyze the data, *$p < 0.05$, **$p < 0.01$ and ***$p < 0.001$).

upregulated and 612 genes downregulated at the false discovery rate 5% (Figure 2A). Among differentially expressed genes, we found 10 upregulated ER stress-related genes in Panc1 (Figure 2B) and 8 upregulated ER stress-related genes in MT5 cell line (Figure 2C). We saw similar trends in the tomatidine-treated human and murine cells with an upregulation in TRIB3 in human (fold change (FC) 1.593, false discovery rate (FDR) 1.62e-05) and mouse (FC 2.157, FDR 5.59e-18), a protein expressed in nucleus that has been known to influence, control, and compensate increased ATF4 expression.[33,34] A notable difference from the murine MT5 cells is the increased expression of NUPR1 in the human Panc1 cells, with a fold change of 3.542 and an FDR of 2.74e-13, which is a critical regulator of the antioxidant system and involved in different cell death pathways including the ER stress pathway.[11,35,36] With the RNA-sequencing results suggesting that the modulation of ER stress-related proteins and previous work implicating tomatidine may impact ATF4, we went on to investigate ATF4-dependent signaling in PDAC. We used ingenuity pathway analysis (IPA) on our dataset to assess gene expression pathways involved. IPA evaluated the upstream gene analysis for ATF4 showcasing the genes that ATF4 interacts with directly and therefore ATF4 can either

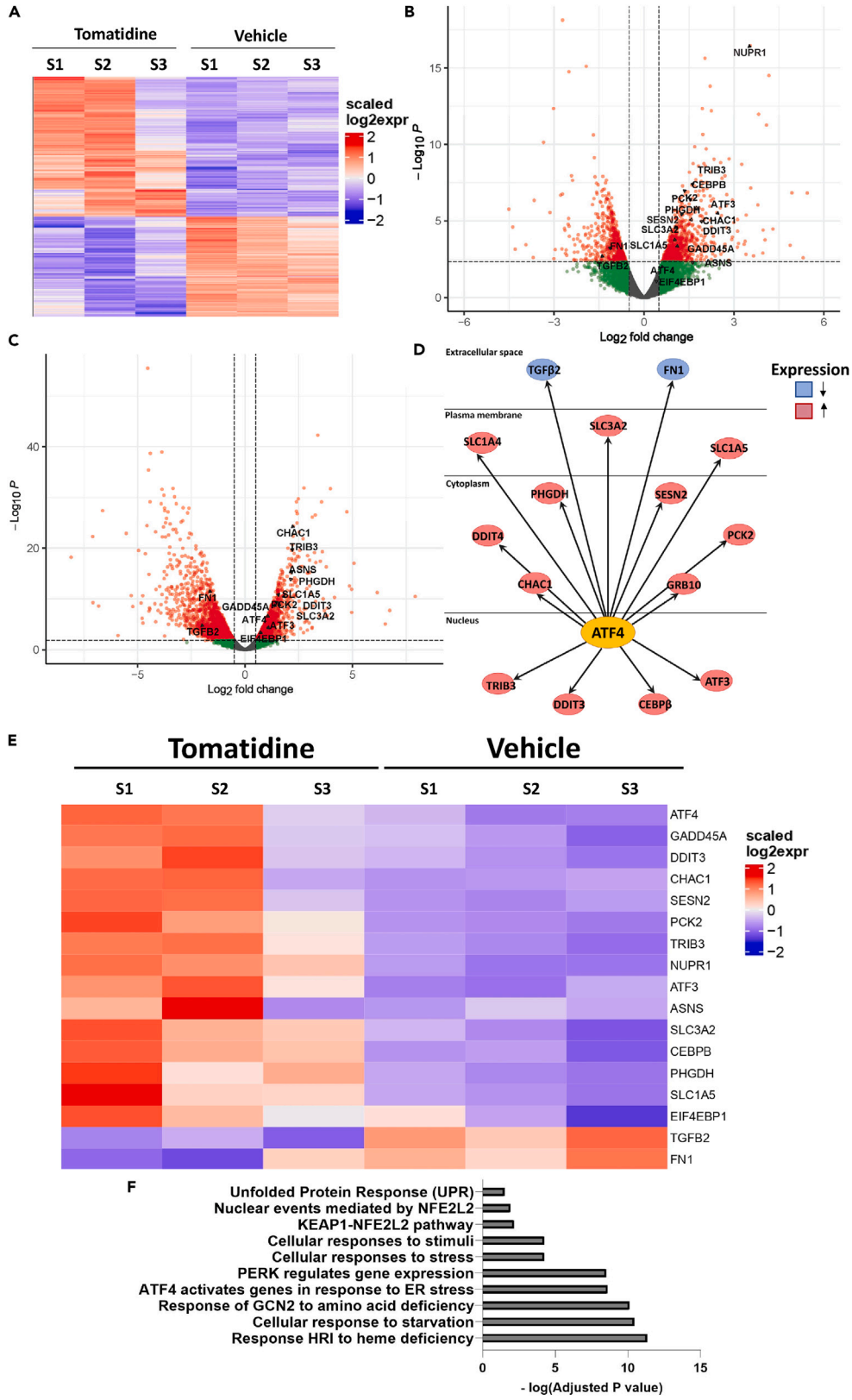
A
Tomatidine
Vehicle
S1
S2
S3
S1
S2
S3
scaled
log2expr
2
1
0
−1
−2
B
−Log10 P
Log2 fold change
NUPR1
TRIB3
CEBPB
PCK2
PHGDM
ATF3
SESN2
CHAC1
SLC3A2
DDIT3
FN1
SLC1A5
GADD45A
TGFB2
ATF4
ASNS
EIF4EBP1
C
−Log10 P
Log2 fold change
CHAC1
TRIB3
ASNS
PHGDH
FN1
SLC1A5
GADD45A
PCK2
DDIT3
ATF4
SLC3A2
ATF3
TGFB2
EIF4EBP1
D
Extracellular space
Plasma membrane
Cytoplasm
Nucleus
Expression
TGFβ2
FN1
SLC3A2
SLC1A4
SLC1A5
PHGDH
SESN2
DDIT4
PCK2
CHAC1
GRB10
ATF4
TRIB3
ATF3
DDIT3
CEBPβ
E
Tomatidine
Vehicle
S1
S2
S3
S1
S2
S3
ATF4
GADD45A
DDIT3
CHAC1
SESN2
PCK2
TRIB3
NUPR1
ATF3
ASNS
SLC3A2
CEBPB
PHGDH
SLC1A5
EIF4EBP1
TGFB2
FN1
scaled
log2expr
2
1
0
−1
−2
F
Unfolded Protein Response (UPR)
Nuclear events mediated by NFE2L2
KEAP1-NFE2L2 pathway
Cellular responses to stimuli
Cellular responses to stress
PERK regulates gene expression
ATF4 activates genes in response to ER stress
Response of GCN2 to amino acid deficiency
Cellular response to starvation
Response HRI to heme deficiency
- log(Adjusted P value)

Figure 2. RNA sequencing reveals that tomatidine modulates ATF4-dependent ER stress genes in pancreatic cancer cells

Human and murine PDAC cell lines were treated for 40 h with 6.4 μg/mL tomatidine, RNA was isolated, and RNA sequencing was performed to analyze differences in gene regulation. N = 3 biological separate experiments.

(A–D) (A) Heatmap of all genes and how they change in tomatidine-treated vs. untreated cells for Panc1 cells (FDR<0.05). Volcano plot highlighting ER stress-related genes in (B) Panc1 and (C) MT5 cells. (Upregulated genes on the right of the central axis and vice versa with higher fold change as we go away from the origin on y axis) (D) IPA upstream analysis of ATF4-related genes in Panc1 cells.

(E) Heatmap elucidating targeting of ATF4-related genes in treated vs. untreated Panc1 cells. (Fold change: +2.5 to −1.5; FDR<0.03).

(F) Top 10 pathways focusing on UPR, ATF4, and ER stress via Reactome analysis of the RNA-sequencing data of treated vs. untreated samples for Panc1 cells. (FDR< 0.03).

upregulate (in red) or downregulate (in blue) their expression (Figure 2D). To further understand this, a heatmap illustrating significant enrichment of genes known to be regulated via ATF4 was investigated. With a threshold cutoff for FDR of 0.03, genes associated with ATF4 activity in tomatidine-treated Panc1 cells are shown (Figure 2E). We found that Panc1 cells treated with tomatidine resulted in an increase in ATF4 and genes it is known to heterodimerize with and/affect transcription of, including CEBPβ, GADD45A, eIF4EBP1, ASNS, and DDIT3 (CHOP). Further, CHAC1, SLC3A2, and SLC1A5 that serve as connection to ATF4 and avoiding cancer cell death pathways are also significantly upregulated. TGF-β2 and FN1 are significantly downregulated in the tomatidine-treated samples with a fold change of −1.3 and −1.6, respectively. Further, the fold change for ATF4 and these associated genes along with their FDR was uploaded to the Reactome pathway analysis to assess their relationship, significance, and false discovery rate. The top 10 relevant hits reveal ATF4 and ER stress pathways being significantly affected after tomatidine administration with a threshold cutoff for FDR = 0.032 (Figure 2F). The pathway "ATF4 activates genes in response to endoplasmic reticulum stress" (8/138 genes, FDR = 5.34e-11; Pathway ID: R-HSA-380994), "PERK regulates gene expression" (8/146 genes, FDR = 8.31e-11; Pathway ID: R-HSA-381042), and "Unfolded Protein Response (UPR)" (8/1503 genes, FDR = 0.032; Pathway ID: R-HSA-381119) indicates that tomatidine administration leads to transcriptomic changes targeting the ATF4-dependent signaling pathway.

ATF4 expression in the PDAC tumor microenvironment

We utilized Kaplan-Meier plotter to examine overall survival of Grade III PDAC patients stratified on the median for ATF4 mRNA expression based on RNA-sequencing data of the PanCancer Database (Figures 3A and 3B). With a median survival of 19.73 months for low expression cohort and 9.73 months for the high expression cohort (p value 0.0068; FDR 20%), these data are congruent with recently published data in PDAC, showing high ATF4 expression to be associated with worse overall and progression-free survival.[14] Further, using a single-cell RNA-sequencing dataset obtained from NIH dbGAP,[37] we discovered elevated ATF4 expression in multiple compartments of the pancreatic tumor microenvironment (TME) including epithelial, stroma, and myeloid immune cells (Figures 3C and 3D). Additionally, we identified ATF4 expression using multiplex immunofluorescence in the tumor microenvironment of genetically engineered mouse model (KrasLSL−G12D, Trp53LSL−R270H, and Pdx1-cre) of PDAC (Figure 3E). With reports indicating that tomatidine can inhibit ATF4-dependent signaling and our RNA-sequencing data, we wanted to investigate how tomatidine can affect ATF4 expression and function in PDAC.

Tomatidine inhibits ATF4-dependent signaling *in vitro*

During stress responses, ATF4 activates downstream proteins such as 4EBP1 and the transcription factor CHOP to balance between survival and apoptotic decisions in normal cells, respectively.[7,38,39] To determine the role of ATF4-dependent signaling, we collected lysates from tomatidine-treated MiaPaca-2 cells and immunoblotted for ATF4 (Figure 4A) and downstream pathway activity (p-4EBP1 and 4EBP1). We observe that activation of downstream proteins of ATF4 (p-4EBP1/4EBP1) is reduced when pancreatic cancer cells are treated with tomatidine in a dose-dependent manner (Figure 4B). Interestingly, tomatidine treatment of tumor cells *in vitro* had no effect on ATF4 protein expression in Figure 4A suggesting that the compound had a primary effect on its activity. To test ATF4 activity, we utilized immunofluorescence and chromatin immunoprecipitation to confirm whether tomatidine affected the ability of ATF4 to function as a transcription factor. As a transcription factor, it is imperative for ATF4 to translocate inside nucleus, bind with downstream genes to function, and render cancer cells a survival benefit. Our immunofluorescence data show that translocation of ATF4 to the nucleus was impaired when pancreatic tumor cells

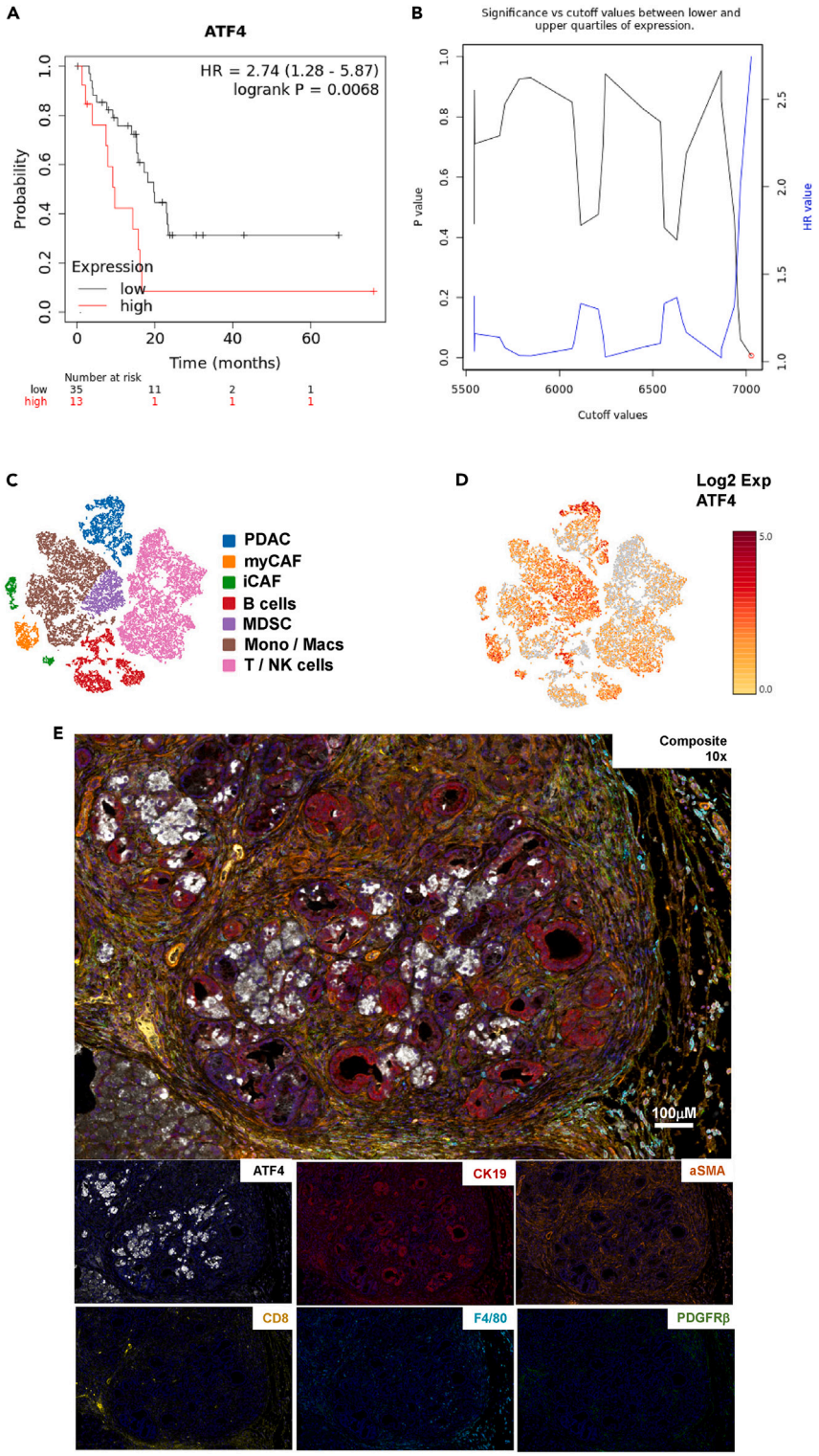

Figure 3. ATF4 expression in PDAC

(A) KM plotter was utilized to examine ATF4 expression in human PDAC specimens examining high vs. low expression compared to overall survival.

(B) Data distribution elucidating significance of the overall survival curve prepared by KM Plotter.

Figure 3. *Continued*
(C and D) (C) scRNA-seq datasets of pancreatic cancer tissue from metastatic patients were obtained from NIH dbGAP (accession phs002045.v1.p1) and (D) analyzed for ATF4 expression. (See also Table S1).
(E) Pancreatic tumor tissue from KPC mice were stained by multiplex IF and imaged using Akoya Vectra Polaris and the Phenochart software to analyze ATF4 in multiple cellular compartments. Markers used to determine ATF4 (white), epithelial cells (CK19; red), stroma (αSMA; orange and PDGFRβ; Green), CD8 T+ cells (yellow), and macrophages (F4/80; turquoise). Scale bar = 100 μm.

were treated with tomatidine (Figures 4C and 4D). Additionally, we discovered that presence of tomatidine reduces the ability of ATF4 to bind promoter regions of downstream genes (Figures 4E, 4F, and 4G). These data suggest that tomatidine is indeed targeting ATF4 *in vitro*.

Tomatidine inhibits pancreatic tumor growth *in vivo*

We wanted to investigate whether tomatidine can be efficacious in reducing tumor burden in a mouse model of PDAC. Daily administration of tomatidine (5 mg/kg) to a subcutaneous model of MT5 pancreatic tumor-bearing C57BL/6 mice resulted in a significant decrease in tumor growth compared to 40% 2-hydroxypropyl-β-cyclodextrin (vehicle)-treated mice (Figure 5A). Further, evaluation of RNA expression isolated from the tumors of the mice showed significantly reduced expression of ATF4 (Figure 5B) and eIF4EBP1 (Figure 5C) mRNA in tomatidine-treated mice compared to vehicle control.

Tomatidine enhances PDAC sensitivity to gemcitabine

ATF4 overexpression has been elucidated as one of the causes of gemcitabine resistance. We hypothesized that tomatidine can enhance gemcitabine chemosensitivity such that lower gemcitabine doses are required for having an antitumor effect in pancreatic cancer. We used MTT assay to assess changes in viability of pancreatic cancer cells treated with combination doses of gemcitabine and tomatidine. We observed that a lower than IC50 dose of tomatidine (3.2 μg/mL) can sufficiently enhance chemosensitivity of gemcitabine in Panc1 (Figure 6A) and MiaPaca-2 (Figure 6B) cells, reducing the IC50 of gemcitabine by ~10-fold in comparison to gemcitabine single-agent treatment. After investigating efficacy of tomatidine as an anticancer agent in PDAC in 2D cell culture and subcutaneous *in vivo* models, we were interested in learning whether the efficacy holds in 3D cell culture and orthotopic tumor models *in vivo*. 3D ECM-hydrogels were utilized to form organoid-like structures and investigate effectivity of tomatidine to inhibit pancreatic tumor growth in a 3D setting (Figure 6C). Four times of the IC50 dose of tomatidine used in 2D monolayer cell culture (28 μg/mL) is required to see inhibition of tumor growth in 3D organoid-like culture (Figure 6D). This observation is in line with reports from other groups looking at reduction of chemotherapy efficacy in 3D cultures.[40] Moreover, we see that the effective tomatidine dose of 28 μg/mL in 3D culture is still able to enhance gemcitabine chemosensitivity similar to our observations in 2D culture (Figure 6E). We then injected luciferase-expressing KPC-derived murine PDAC cells into the pancreas of C57BL/6 mice orthotopically and administered 5 mg/kg single-agent tomatidine daily or 10 mg/kg single-agent gemcitabine twice per week or in combination (Figure 6F). In comparison to vehicle, single-agent tomatidine did not significantly reduce tumor burden unlike previously observed results in subcutaneous tumors in Figure 5. As expected, since mice metabolize gemcitabine more efficiently than humans,[41] single-agent gemcitabine chemotherapy reduces tumor weights compared to vehicle control animals. Combination of tomatidine and gemcitabine treatment did significantly reduce tumor burden at study endpoint compared to single-agent gemcitabine (Figure 6G), reiterating the importance of tomatidine as a feasible anticancer agent to enhance gemcitabine chemosensitivity in PDAC.

Tomatidine induced inhibition of ATF4-dependent signaling induces ferroptosis in pancreatic cancer cells

RNA sequencing of pancreatic cancer cell lines treated with tomatidine shows upregulation of ER stress-related genes. Additionally, genes relevant for ferroptosis-mediated cell death were a significant top hit via IPA (Figure 7A). This included upregulation of genes implicated in ferroptosis such as SLC3A2 (FC: 1.565, FDR: 3.46E-08)[42,43] and LONP1 (FC: 1.15, FDR: 0.00524).[44] We also saw upregulation in genes such as CHAC1 in Figure 2 that has been previously implicated to be controlled via ATF4 to avoid ferroptosis.[9] Ferroptosis is an iron-dependent type of programmed cell death triggered by failure of antioxidant programs that is characterized by extensive lipid peroxidation leading to eventual cellular demise.[16,45] ATF4 engagement of the integrated stress response can restore cellular redox levels and protect cells from ferroptosis. We show that tomatidine can simultaneously drive mitochondrial biogenesis and induce

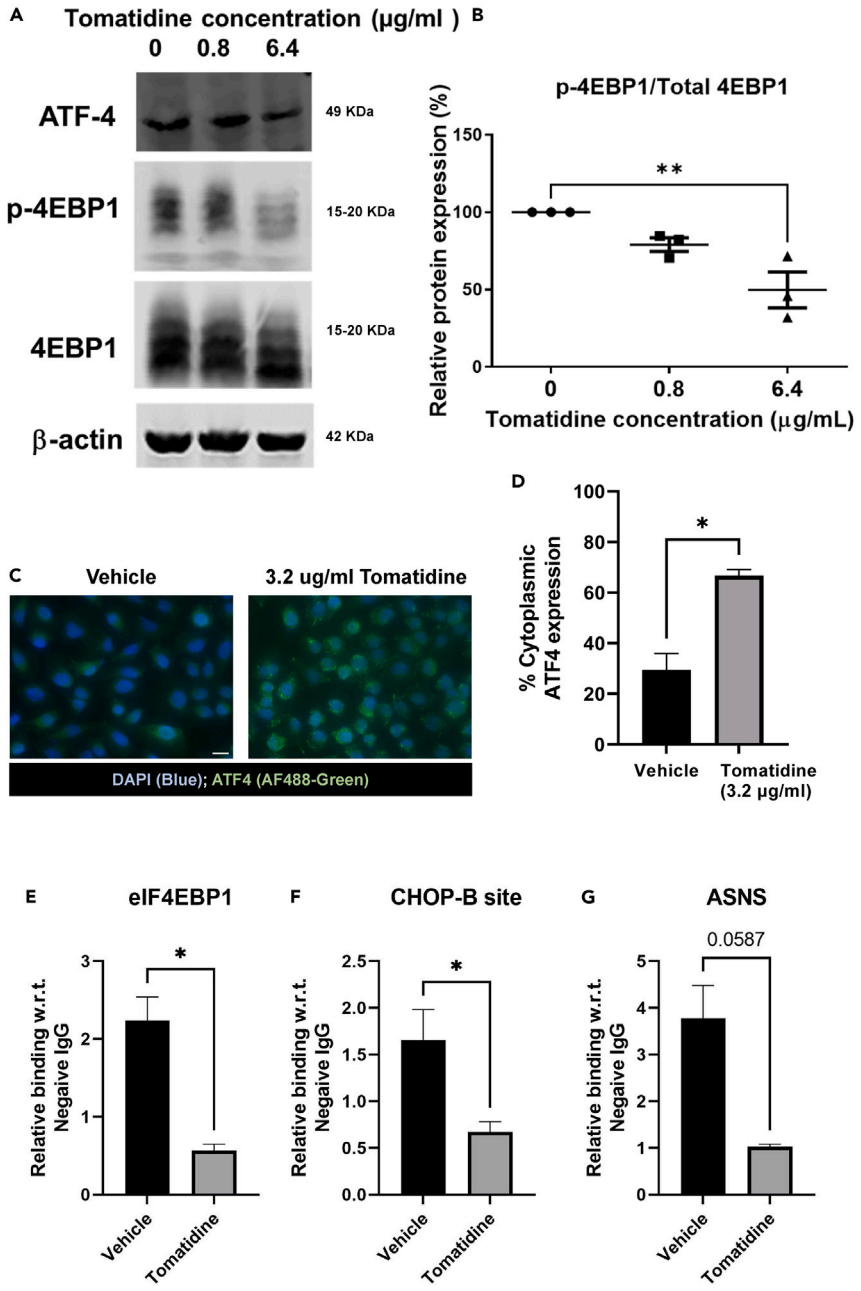

Figure 4. Tomatidine inhibits ATF4-dependent signaling in PDAC

(A and B) (A) MiaPaca-2 tumor cells were treated with tomatidine for 72 h and cell lysates were immunoblotted for ATF4, 4EBP1, and phospho-4EBP1(p-4EBP1) protein expression and (B) p-4EBP1/4EBP1 levels quantified by densitometry.

(C) Immunofluorescence (IF) was performed on vehicle (DMSO) or tomatidine-treated Panc1 cells to track ATF4 (FITC-Green) translocation from nucleus (DAPI-Blue) to cytoplasm. Scale bar = 50 µm.

(D–G) (D) Nuclear to cytoplasmic translocation was quantified. Panc1 cells were treated with vehicle (DMSO) or tomatidine for 40 h and ATF4 transcriptional activity was analyzed by chromatin immunoprecipitation (ChIP) qPCR evaluating binding of ATF4 to the downstream promoter regions of (E) eIF4EBP1 (F) CHOP- B site and (G) ASNS. Data are reported as the means + SEMs. n = 3 or more independent biological replicates (4B, One-way ANOVA with Tukey's test for pairwise comparisons was used to analyze the data; 4D-G, Two-tailed independent student's test was used to analyze the data, *p < 0.05).

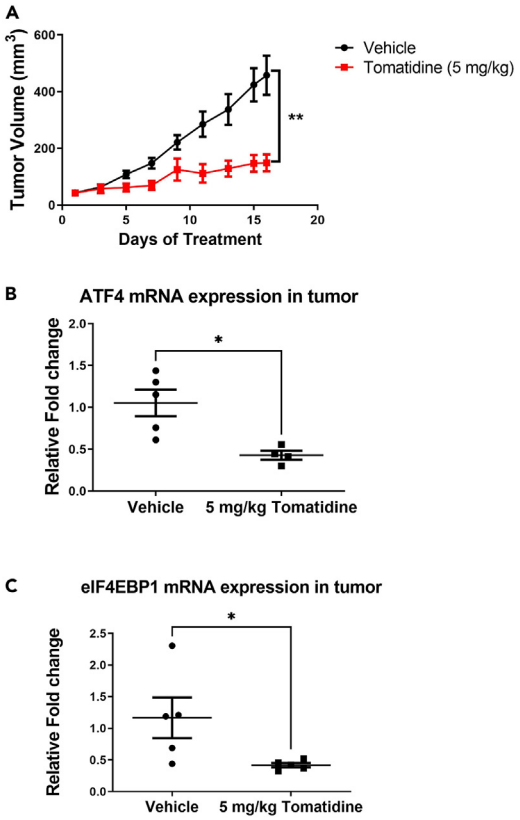

Figure 5. *In vivo* tomatidine treatment inhibits pancreatic tumor growth

(A–C) (A) MT5 tumor-bearing C57BL/6 mice (5 mice/group) were treated with 5 mg/kg daily i.p. injections of tomatidine or vehicle control (40% HPBCD) and monitored for tumor growth. (n = 5/group). RNA isolated from the tumor tissues of MT5 tumor-bearing C57BL/6 mice treated with vehicle or 5 mg/kg daily i.p. injections of tomatidine were assessed for (B) ATF4 and (C) eIF4EBP1 expression via qPCR. Data are reported as the means + SEMs. n = 5 mice per group. (5A, mixed between-within subjects ANOVA shows a significant interaction between days of treatment and group; 5B-C, Two-tailed independent student's test was used to analyze the data, *p < 0.05).

lipid peroxidation, which are hallmarks of ferroptosis. Tomatidine-treated Panc1 and MiaPaca-2 cells induce significant lipid peroxidation compared to vehicle controls as measured by C11 Bodipy staining (Figures 7B and 7C). GPX4 is responsible for negating the lipid ROS that eventually leads to ferroptosis. Interestingly, tomatidine treatment in Panc1 and MiaPaca-2 cells leads to a significant decrease in expression of GPX4 compared to vehicle-treated cells (Figure 7E) suggesting tomatidine can reverse the cancer cell's ability to deal with the oxidative damage and induce ferroptosis. Cancer cells alter their metabolism and mitochondrial function to support their survival as anabolic machines which can be regulated by ATF4 activity.[46] We found that short-term *in vitro* treatment of PDAC cells with tomatidine leads to an increase in basal respiration as well as spare reserve capacity indicative of increased mitochondrial fitness (Figure 7F). These data could indicate the presence of more functional mitochondria leading to more oxidative phosphorylation which generates ROS that can be amplified via the Fenton reaction and drive ferroptosis. Therefore, tomatidine-mediated inhibition of ATF4 signaling can increase sensitivity to ferroptosis-mediated cell death in PDAC (Figure 7G).

DISCUSSION

There is a need for novel alternative therapeutic strategies with fewer toxicities and issues of resistance in treating PDAC. Steroidal alkaloids, with selective toxicity toward cancer cells and reduced issues of therapeutic resistance, are a promising therapeutic approach to treat cancer.[47,48] The aim of this study was to determine whether tomatidine, a steroidal alkaloid metabolite present in tomatoes, can limit pancreatic cancer, and investigate its underlying mechanism of action in the context of pancreatic cancer. We showed that tomatidine can inhibit pancreatic tumor growth in pancreatic cancer cell lines *in vitro*. In addition to our

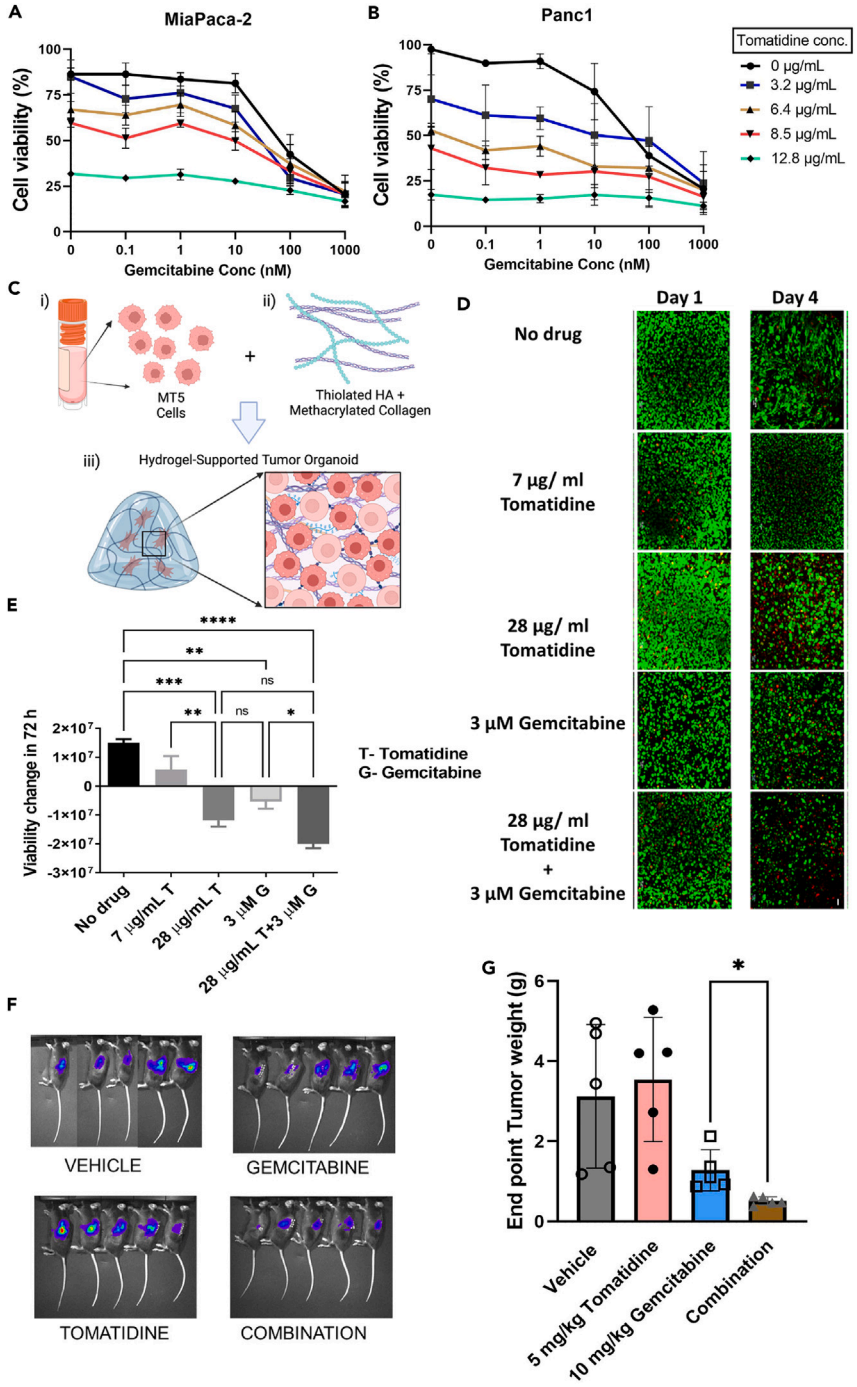

Figure 6. Tomatidine improves PDAC chemosensitivity

(A and B) (A) Panc1 and (B) MiaPaca-2 pancreatic tumor cell lines were treated with increasing concentrations of tomatidine and gemcitabine in combination for 72 h and assayed for cell growth via MTT assay.

(C and D) (C) Murine pancreatic cells (MT5) were grown in extracellular matrix (ECM)-based Collagen-Hyaluronic hydrogels, treated with tomatidine, and (D) Live (green)/Dead (red) assay was performed and imaged by confocal microscopy. Scale bar = 50 µm.

(E) ATP activity was measured via Cell Glo Titer assay and used to measure cell viability in 3D cultures.

Figure 6. *Continued*
(F and G) (F) KPC-luc tumor cells were orthotopically injected in the pancreas of C57BL/6 mice and treated with 5 mg/kg daily i.p. injections of tomatidine or 10 mg/kg gemcitabine twice a week or both in combination and (G) evaluated for tumor burden in comparison to vehicle control at study endpoint. Data are reported as the means + SEMs. n = 3 or more independent biological replicates. (6E, One-way ANOVA with Tukey's test for pairwise comparisons was used to analyze the data; 6G, Two-tailed independent student's test was used to analyze the data, *$p < 0.05$ **$p < 0.003$).

in vitro studies, we found tomatidine can significantly reduce pancreatic tumor growth in C57BL/6 mice subcutaneously injected with murine pancreatic cancer cells and in combination with gemcitabine in more aggressive orthotopic tumor models. This is the first report to provide evidence that tomatidine can affect the growth and survival of pancreatic epithelial tumor cells.

Reports by investigators in disease settings other than cancer have associated tomatidine with inhibition of ATF4-dependent signaling. Tomatidine was shown as a potential agent and/or lead compound for reducing ATF4 activity, weakness, and atrophy in aged skeletal muscle.[31,32] Further, tomatidine was shown to downregulate ATF4 expression to exert antiviral properties to all DENV viral serotypes and inhibit viral particle production.[49] Tomatidine has further been linked to ameliorating endoplasmic reticulum stress and inhibiting ATF4 expression to inhibit tumor necrosis factor-α-induced apoptosis in C_2C_{12} myoblasts.[50] However, these reports show correlative evidence to indicate tomatidine can target ATF4 and direct interaction of tomatidine and ATF4-dependent signaling is unclear and needed investigation. Further, there are no reports of how tomatidine affects pancreatic cancer. In this study, we show that tomatidine can inhibit protein expression of 4EBP1 which has been implicated to help tumor cells survive via ATF4 expression. We show that tomatidine can affect binding of ATF4 with its downstream genes such as eIF4EBP1, ASNS, and CHOP via chromatin immunoprecipitation. We further provide evidence that tomatidine can reduce engagement of ATF4 inside the nucleus and instead shuttle ATF4 out to the cytoplasm in an aggregate-like droplet. ATF4, being a transcription factor, has been reported to require binding as a homodimer or heterodimer with CARE/CRE promoter elements to properly function and alleviate cellular stress.[51] This study is the first report of tomatidine affecting the binding activity of the transcription factor, causing hindrances in proper functioning of ATF4. This implicates tomatidine as a potential compound to attenuate ATF4 activity in PDAC. There are no currently known drugs against ATF4 directly. PERK inhibitors and ISR inhibitors[11,52] can potentiate ATF4 activity indirectly by affecting upstream proteins PERK and eIF2α. However, PERK ablation can have extremely toxic effects and cause pancreatic injury. Reports indicate activation of type 1 interferon signaling occurs upon PERK ablation and is responsible for pancreatic injury and the loss of exocrine and endocrine tissues and functions.[53] We observed no apparent toxicities when treating animals with tomatidine *in vivo* (data not shown). These difficulties observed in clinical and preclinical trials of PERK inhibitors that target the upstream elements of ATF4 can be mitigated by inhibiting ATF4 directly. Further, this study also highlights the importance of drug testing beyond 2D cell culture or subcutaneous tumor systems. Through analyzing tomatidine efficacy in 3D cell culture and orthotopic mice models, we realize that higher doses of tomatidine is required to have a similar effect observed in 2D and subcutaneous tumor model systems of pancreatic cancer. This could be simply due to the need for diffusion to enable transport of the therapeutic agents into the 3D tumor tissues or could result in deeper genetic and phenotypic changes occurring in the cells upon the transition from 2D to 3D. We have previously demonstrated such shifts in other tumor cell lines and using human patient-derived tumor organoid models.[54,55] Similar to this observation in the 3D cell culture, we observed the lack of inhibition by tomatidine toward the antiproliferative capacity in MiaPaca-2 and Panc1 at a select few lower than IC50 doses in our 2D cell viability assay. However, they do show moderate apoptosis at the same concentrations. This may be due to the less cytotoxic nature of tomatidine and aligns with the fact that tomatidine affects the stress-related transcription factor ATF4. Other reasons for these observations could also be alluded to MTT assay design parameters such as cell density and assay timeline. This also provides an important opportunity to evaluate cell-cell interactions to understand the role of extrinsic ATF4-dependent signaling in the tumor microenvironment and how it is affected by tomatidine in the context of pancreatic cancer. Future investigation in understanding the structure activity relationship of tomatidine can provide information on the binding site of ATF4 such that tomatidine can be derived to improve potency and efficacy and established as an ATF4-targeting drug.

ATF4 overexpression has also been elucidated as the cause of chemotherapy resistance in PDAC. Gemcitabine and other standard-of-care chemotherapies can trigger ER stress pathways which signal cancer cell evolution to persistent cancer cell phenotypes and help them survive and become drug resistant.[11–13] We show that

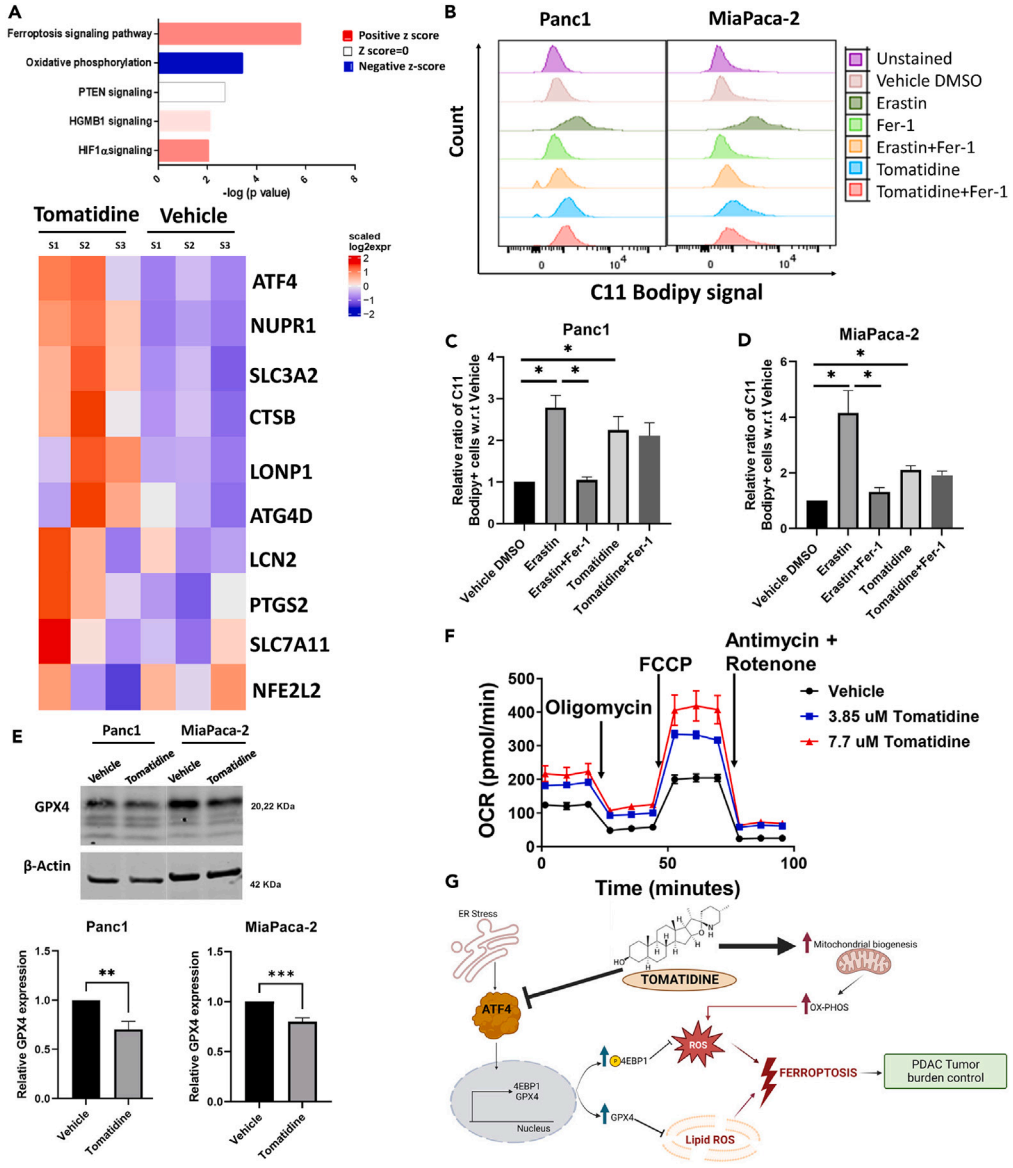

Figure 7. Tomatidine mediated inhibition of ATF4 signaling can increase sensitivity to ferroptotic cell death in PDAC

(A) Panc-1 tumor cells were treated with tomatidine (6.4 μg/mL) and analyzed by RNA sequencing. Ingenuity pathway analysis of the regulated genes suggested ferroptosis as a top hit for tomatidine-treated cells.

(B–D) (B) Pancreatic cancer cells were treated with vehicle (DMSO), erastin (to induce ferroptosis), ferrostatin-1 (to inhibit ferroptosis), tomatidine, or in different combinations and lipid peroxidation of (C) Panc-1 and (D) MiaPaca-2 was analyzed by flow cytometry using Bodipy-11.

(E) Panc-1 and MiaPaca-2 cells treated with vehicle (DMSO) or tomatidine and lysates collected after 24 h were immunoblot for GPX4 expression.

(F) Panc1 cells were plated overnight and treated with tomatidine for 6 h and then assayed by Seahorse assay to analyze mitochondrial fitness.

(G) Schematic showing how tomatidine can regulate ATF4-dependent signaling to induce ferroptosis in pancreatic cancer. Data are reported as the means + SEMs. n = 3 or more independent biological replicates. (7C-D, Two-tailed independent student's test was used to analyze the data; 7F, Two-tailed independent student's test was used to analyze the data, *p < 0.05, **p < 0.007).

tomatidine can enhance gemcitabine chemosensitivity in 2D and 3D cell culture models as well as an orthotopic pancreatic tumor model *in vivo*. Tomatidine was reported to be a potent chemosensitizer in cell culture models against multi-drug resistance study two decades back. Since then, this is the first study to show that tomatidine can enhance chemosensitivity and hence reduce toxicity for standard-of-care chemotherapies both *in vitro* and *in vivo*. The RNA-sequencing analysis outlined in this study also reveals that tomatidine can negatively regulate TGF-β expression. Cancer-associated fibroblasts-mediated ATF4 expression has been implicated to promote malignancy and gemcitabine resistance in pancreatic cancer via the TGF-β1/SMAD2/3 pathway and ABCC1 transactivation.[14] Failure of traditional chemotherapeutics to achieve efficient results in pancreatic cancer is largely attributed to its ability to hijack the immune system.[56] Pancreatic cancer can convert the immune system that attacks tumor cells to a system that supports the cancer by exerting trophic actions. ER stress-induced ATF4 expression has been implied to regulate the function of multiple immune cells in the TME causing a shift to a pro-tumorigenic and immunosuppressive myeloid cell and M2-like macrophage phenotype as well as causing T cell dysfunction.[5,57,58] Future investigations are required to understand the functional interactions undergone by different immune cells residing in the TME when treated with tomatidine and whether ATF4-dependent signaling plays a role in the interactions.

This study is also the first report that shows tomatidine can be a potential inducer of ferroptosis. Ferroptosis is a comparatively newly discovered form of non-apoptotic cell death. Ferroptosis is triggered by increased intracellular iron and ROS and is considered as an option for cancer therapy since a lot of cancers, including pancreatic cancer, exploit iron dependency for survival. We show that tomatidine can induce lipid peroxidation, reduce GPX4 expression, and increase mitochondrial biogenesis leading to ferroptosis in pancreatic cancer cells. This is in line with the observation that tomatidine can accelerate mitochondrial biogenesis in human embryonic stem cell-derived cardiomyocytes.[59] Treatment with ferrostatin-1 (Fer-1), a ferroptosis inhibitor that acts via scavenging and trapping the accumulated ROS, in combination with tomatidine is unable to significantly reverse the lipid peroxidation induced by tomatidine. This is an interesting observation since we observe successful reversal of the induction of lipid ROS when Fer-1 is used in combination with the established ferroptosis inducer erastin. This might be because of the unique chemistry of the small molecule, tomatidine, that hinders the ability of Fer-1 to inhibit ferroptosis or there might be other factors in play that contribute to the C11 Bodipy signal. More studies need to be conducted to understand the exact mechanism of why Fer-1 cannot inhibit the ferroptosis induced via tomatidine. Additionally, there are mechanisms in place to resist ferroptosis. ATF4 engagement of the ISR can restore cellular redox levels and protect from ferroptosis. Drugs like artesunate and dihydroartemisinin can induce ATF4-CHOP-CHAC1 expression in Burkitt's lymphoma and PERK/ATF4/HSPA5 pathway in glioma cells, respectively, to attenuate ferroptosis.[9,21] ATF4 induction secondary to the stress response triggered by MESH1 silencing is also sufficient to attenuate ferroptosis in renal cell carcinoma cells.[60] Similarly, constitutive ATF4 signaling protects renal cell carcinoma cells from ferroptosis induced by sorafenib.[20] In PDAC, ATF4-induced HSPA5 has been elucidated as the cause of desensitizing cells to ferroptotic cell death.[61] Therefore, ATF4-dependent signaling is an important mechanism to protect cells from ferroptosis, drive tumorigenesis, and induce chemoresistance. Targeting of ATF4 via tomatidine can potentially sensitize pancreatic cancer cells to ferroptosis-mediated cancer cell death.

Overall, the work outlined in this study sets up a basic understanding of the mechanism of action of tomatidine in limiting pancreatic tumor growth and tests its effectiveness in pancreatic tumor-bearing *in vivo* models for proof of principle. This study sheds light on a novel plant-derived anticancer treatment that targets an upregulated pathway (ATF4-dependent signaling) in pancreatic cancer. Data here support the development of tomatidine-based derivatives that could lead to novel and new therapeutic strategies for targeting the tumor via cellular stress pathways.

Limitations of the study

Although we have tested tomatidine in relevant preclinical models of pancreatic cancer, effectiveness of tomatidine as an anticancer agent needs to be tested in genetically engineered mouse models of spontaneously arising pancreatic cancer. Further characterization of how tomatidine affects the stroma and immune microenvironment of tomatidine will also be required to further study the feasibility of tomatidine as a candidate agent targeting PDAC.

STAR★METHODS

Detailed methods are provided in the online version of this paper and include the following:

SUPPLEMENTAL INFORMATION

Supplemental information can be found online at https://doi.org/10.1016/j.isci.2023.107408.

ACKNOWLEDGMENTS

The project described was in part funded by OSUCCC Cure for Pancreatic Cancer Development Fund. Research reported in this publication was supported by The Ohio State University Comprehensive Cancer Center (OSUCCC) and the National Institutes of Health (NIH) under grant P30CA016058. Research was supported from the Pelotonia Graduate Fellowship Program. This research was made possible through resources, expertise, and support provided by the Pelotonia Institute for Immuno-Oncology (PIIO), which is funded by the Pelotonia community and the OSUCCC. We also thank K. Das from the Immune Monitoring and Discovery Platform (IMDP) of the Pelotonia Institute for Immuno-Oncology (PIIO) for technical support. We thank OSUCCC shared resources Analytical Cytometry, Genomics, Bioinformatics and Clinical and Translational Sciences Shared Resources and University Laboratory Animal Resources. We used BioRender to generate select schematics.

AUTHOR CONTRIBUTIONS

D.M. and T.A.M. conceived and designed the study. D.M., S.C., L.B., L.D., J.W., S.J., M.T., T.P., H.L., and A.G. conducted the experiments. A.S. provided supervision on 3D ECM-hydrogel studies. A.M.S. provided expertise on seahorse studies. M.P. performed computational analyses for RNA sequencing. J.M. and T.L.F. provided methodology and resources for multiplex IF. D.A. and J.R.F. provided expertise on chemical reagents and steroidal alkaloid chemistry. S.C. performed statistical analysis on raw data. D.M. wrote the manuscript, which was reviewed and edited by all co-authors. All authors read and approved the final manuscript.

DECLARATION OF INTERESTS

Authors declare that they have no potential conflicts of interest.

INCLUSION AND DIVERSITY

We support inclusive, diverse, and equitable conduct of research.

Received: April 5, 2023
Revised: June 19, 2023
Accepted: July 13, 2023
Published: July 17, 2023

REFERENCES

1. Siegel, R.L., Miller, K.D., Wagle, N.S., and Jemal, A. (2023). Cancer statistics, 2023. Ca - Cancer J. Clin. *73*, 17–48. https://doi.org/10.3322/caac.21763.

2. Janssen, Q.P., O'Reilly, E.M., van Eijck, C.H.J., and Groot Koerkamp, B. (2020). Neoadjuvant Treatment in Patients With Resectable and Borderline Resectable Pancreatic Cancer. Front. Oncol. *10*, 41. https://doi.org/10.3389/fonc.2020.00041.

3. Lopez, N.E., Prendergast, C., and Lowy, A.M. (2014). Borderline resectable pancreatic cancer: definitions and management. World J. Gastroenterol. *20*, 10740–10751. https://doi.org/10.3748/wjg.v20.i31.10740.

4. Ameri, K., and Harris, A.L. (2008). Activating transcription factor 4. Int. J. Biochem. Cell Biol. *40*, 14–21. https://doi.org/10.1016/j.biocel.2007.01.020.

5. Mukherjee, D., Bercz, L.S., Torok, M.A., and Mace, T.A. (2020). Regulation of cellular immunity by activating transcription factor 4. Immunol. Lett. *228*, 24–34. https://doi.org/10.1016/j.imlet.2020.09.006.

6. Yamaguchi, S., Ishihara, H., Yamada, T., Tamura, A., Usui, M., Tominaga, R., Munakata, Y., Satake, C., Katagiri, H., Tashiro, F., et al. (2008). ATF4-mediated induction of 4E-BP1 contributes to pancreatic beta cell survival under endoplasmic reticulum stress. Cell Metabol. *7*, 269–276. https://doi.org/10.1016/j.cmet.2008.01.008.

7. Tameire, F., Verginadis, I.I., Leli, N.M., Polte, C., Conn, C.S., Ojha, R., Salas Salinas, C., Chinga, F., Monroy, A.M., Fu, W., et al. (2019). ATF4 couples MYC-dependent translational activity to bioenergetic demands during tumour progression. Nat. Cell Biol. *21*, 889–899. https://doi.org/10.1038/s41556-019-0347-9.

8. Cao, Y., Trillo-Tinoco, J., Sierra, R.A., Anadon, C., Dai, W., Mohamed, E., Cen, L., Costich, T.L., Magliocco, A., Marchion, D., et al. (2019). ER stress-induced mediator C/EBP homologous protein thwarts effector T cell activity in tumors through T-bet repression. Nat. Commun. *10*, 1280. https://doi.org/10.1038/s41467-019-09263-1.

9. Wang, N., Zeng, G.Z., Yin, J.L., and Bian, Z.X. (2019). Artesunate activates the ATF4-CHOP-CHAC1 pathway and affects ferroptosis in Burkitt's Lymphoma. Biochem. Biophys. Res. Commun. *519*, 533–539. https://doi.org/10.1016/j.bbrc.2019.09.023.

10. Rozpedek, W., Pytel, D., Mucha, B., Leszczynska, H., Diehl, J.A., and Majsterek, I. (2016). The Role of the PERK/eIF2alpha/ATF4/CHOP Signaling Pathway in Tumor Progression During Endoplasmic Reticulum Stress. Curr. Mol. Med. *16*, 533–544. https://doi.org/10.2174/1566524016666160523143937.

11. Palam, L.R., Gore, J., Craven, K.E., Wilson, J.L., and Korc, M. (2015). Integrated stress response is critical for gemcitabine resistance in pancreatic ductal adenocarcinoma. Cell Death Dis. *6*, e1913. https://doi.org/10.1038/cddis.2015.264.

12. Tadros, S., Shukla, S.K., King, R.J., Gunda, V., Vernucci, E., Abrego, J., Chaika, N.V., Yu, F., Lazenby, A.J., Berim, L., et al. (2017). De Novo Lipid Synthesis Facilitates Gemcitabine Resistance through Endoplasmic Reticulum Stress in Pancreatic Cancer. Cancer Res. *77*, 5503–5517. https://doi.org/10.1158/0008-5472.CAN-16-3062.

13. Wang, L., Zhang, Y., Wang, W., Zhu, Y., Chen, Y., and Tian, B. (2017). Gemcitabine treatment induces endoplasmic reticular (ER) stress and subsequently upregulates urokinase plasminogen activator (uPA) to block mitochondrial-dependent apoptosis in Panc-1 cancer stem-like cells (CSCs). PLoS One *12*, e0184110. https://doi.org/10.1371/journal.pone.0184110.

14. Wei, L., Lin, Q., Lu, Y., Li, G., Huang, L., Fu, Z., Chen, R., and Zhou, Q. (2021). Cancer-associated fibroblasts-mediated ATF4 expression promotes malignancy and gemcitabine resistance in pancreatic cancer via the TGF-beta1/SMAD2/3 pathway and ABCC1 transactivation. Cell Death Dis. *12*, 334. https://doi.org/10.1038/s41419-021-03574-2.

15. Tait, S.W.G., Ichim, G., and Green, D.R. (2014). Die another way–non-apoptotic mechanisms of cell death. J. Cell Sci. *127*, 2135–2144. https://doi.org/10.1242/jcs.093575.

16. Dixon, S.J., Lemberg, K.M., Lamprecht, M.R., Skouta, R., Zaitsev, E.M., Gleason, C.E., Patel, D.N., Bauer, A.J., Cantley, A.M., Yang, W.S., et al. (2012). Ferroptosis: an iron-dependent form of nonapoptotic cell death. Cell *149*, 1060–1072. https://doi.org/10.1016/j.cell.2012.03.042.

17. Nie, Z., Chen, M., Gao, Y., Huang, D., Cao, H., Peng, Y., Guo, N., Wang, F., and Zhang, S. (2022). Ferroptosis and Tumor Drug Resistance: Current Status and Major Challenges. Front. Pharmacol. *13*, 879317. https://doi.org/10.3389/fphar.2022.879317.

18. Zhang, C., Liu, X., Jin, S., Chen, Y., and Guo, R. (2022). Ferroptosis in cancer therapy: a novel approach to reversing drug resistance. Mol. Cancer *21*, 47. https://doi.org/10.1186/s12943-022-01530-y.

19. Li, J., Cao, F., Yin, H.L., Huang, Z.J., Lin, Z.T., Mao, N., Sun, B., and Wang, G. (2020). Ferroptosis: past, present and future. Cell Death Dis. *11*, 88. https://doi.org/10.1038/s41419-020-2298-2.

20. Gao, R., Kalathur, R.K.R., Coto-Llerena, M., Ercan, C., Buechel, D., Shuang, S., Piscuoglio, S., Dill, M.T., Camargo, F.D., Christofori, G., and Tang, F. (2021). YAP/TAZ and ATF4 drive resistance to Sorafenib in hepatocellular carcinoma by preventing ferroptosis. EMBO Mol. Med. *13*, e14351. https://doi.org/10.15252/emmm.202114351.

21. Chen, Y., Mi, Y., Zhang, X., Ma, Q., Song, Y., Zhang, L., Wang, D., Xing, J., Hou, B., Li, H., et al. (2019). Dihydroartemisinin-induced unfolded protein response feedback attenuates ferroptosis via PERK/ATF4/HSPA5 pathway in glioma cells. J. Exp. Clin. Cancer Res. *38*, 402. https://doi.org/10.1186/s13046-019-1413-7.

22. Gielecinska, A., Kciuk, M., Mujwar, S., Celik, I., Kolat, D., Kaluzinska-Kolat, Z., and Kontek, R. (2023). Substances of Natural Origin in Medicine: Plants vs. Cancer. Cells *12*. https://doi.org/10.3390/cells12070986.

23. Sharifi-Rad, J., Ozleyen, A., Boyunegmez Tumer, T., Oluwaseun Adetunji, C., El Omari, N., Balahbib, A., Taheri, Y., Bouyahya, A., Martorell, M., Martins, N., and Cho, W.C. (2019). Natural Products and Synthetic Analogs as a Source of Antitumor Drugs. Biomolecules *9*, 679. https://doi.org/10.3390/biom9110679.

24. Bailly, C. (2021). The steroidal alkaloids alpha-tomatine and tomatidine: Panorama of their mode of action and pharmacological properties. Steroids *176*, 108933. https://doi.org/10.1016/j.steroids.2021.108933.

25. Friedman, M., Henika, P.R., and Mackey, B.E. (1996). Feeding of potato, tomato and eggplant alkaloids affects food consumption and body and liver weights in mice. J. Nutr. *126*, 989–999. https://doi.org/10.1093/jn/126.4.989.

26. Friedman, M., Henika, P.R., and Mackey, B.E. (2003). Effect of feeding solanidine, solasodine and tomatidine to non-pregnant and pregnant mice. Food Chem. Toxicol. *41*, 61–71. https://doi.org/10.1016/s0278-6915(02)00205-3.

27. Friedman, M., Levin, C.E., Lee, S.U., Kim, H.J., Lee, I.S., Byun, J.O., and Kozukue, N. (2009). Tomatine-containing green tomato extracts inhibit growth of human breast, colon, liver, and stomach cancer cells. J. Agric. Food Chem. *57*, 5727–5733. https://doi.org/10.1021/jf900364j.

28. Friedman, M. (2013). Anticarcinogenic, cardioprotective, and other health benefits of tomato compounds lycopene, alpha-tomatine, and tomatidine in pure form and in fresh and processed tomatoes. J. Agric. Food

Chem. *61*, 9534–9550. https://doi.org/10.1021/jf402654e.

29. Yan, K.H., Lee, L.M., Yan, S.H., Huang, H.C., Li, C.C., Lin, H.T., and Chen, P.S. (2013). Tomatidine inhibits invasion of human lung adenocarcinoma cell A549 by reducing matrix metalloproteinases expression. Chem. Biol. Interact. *203*, 580–587. https://doi.org/10.1016/j.cbi.2013.03.016.

30. Wang, B.S., Liu, Z., Sun, S.L., and Zhao, Y. (2014). Identification of genes and candidate agents associated with pancreatic cancer. Tumour Biol. *35*, 81–88. https://doi.org/10.1007/s13277-013-1009-3.

31. Dyle, M.C., Ebert, S.M., Cook, D.P., Kunkel, S.D., Fox, D.K., Bongers, K.S., Bullard, S.A., Dierdorff, J.M., and Adams, C.M. (2014). Systems-based discovery of tomatidine as a natural small molecule inhibitor of skeletal muscle atrophy. J. Biol. Chem. *289*, 14913–14924. https://doi.org/10.1074/jbc.M114.556241.

32. Ebert, S.M., Dyle, M.C., Bullard, S.A., Dierdorff, J.M., Murry, D.J., Fox, D.K., Bongers, K.S., Lira, V.A., Meyerholz, D.K., Talley, J.J., and Adams, C.M. (2015). Identification and Small Molecule Inhibition of an Activating Transcription Factor 4 (ATF4)-dependent Pathway to Age-related Skeletal Muscle Weakness and Atrophy. J. Biol. Chem. *290*, 25497–25511. https://doi.org/10.1074/jbc.M115.681445.

33. He, X., Wu, D., Xu, Y., Zhang, Y., Sun, Y., Chang, X., Zhu, Y., and Tang, W. (2022). Perfluorooctanoic acid promotes pancreatic beta cell dysfunction and apoptosis through ER stress and the ATF4/CHOP/TRIB3 pathway. Environ. Sci. Pollut. Res. Int. *29*, 84532–84545. https://doi.org/10.1007/s11356-022-21188-9.

34. Örd, T., Örd, D., Kaikkonen, M.U., and Örd, T. (2021). Pharmacological or TRIB3-Mediated Suppression of ATF4 Transcriptional Activity Promotes Hepatoma Cell Resistance to Proteasome Inhibitor Bortezomib. Cancers *13*, 2341. https://doi.org/10.3390/cancers13102341.

35. Huang, C., Santofimia-Castaño, P., and Iovanna, J. (2021). NUPR1: A Critical Regulator of the Antioxidant System. Cancers *13*, 3670. https://doi.org/10.3390/cancers13153670.

36. Santofimia-Castaño, P., Lan, W., Bintz, J., Gayet, O., Carrier, A., Lomberk, G., Neira, J.L., González, A., Urrutia, R., Soubeyran, P., and Iovanna, J. (2018). Inactivation of NUPR1 promotes cell death by coupling ER-stress responses with necrosis. Sci. Rep. *8*, 16999. https://doi.org/10.1038/s41598-018-35020-3.

37. Elyada, E., Bolisetty, M., Laise, P., Flynn, W.F., Courtois, E.T., Burkhart, R.A., Teinor, J.A., Belleau, P., Biffi, G., Lucito, M.S., et al. (2019). Cross-Species Single-Cell Analysis of Pancreatic Ductal Adenocarcinoma Reveals Antigen-Presenting Cancer-Associated Fibroblasts. Cancer Discov. *9*, 1102–1123. https://doi.org/10.1158/2159-8290.CD-19-0094.

38. Gingras, A.C., Gygi, S.P., Raught, B., Polakiewicz, R.D., Abraham, R.T., Hoekstra, M.F., Aebersold, R., and Sonenberg, N. (1999). Regulation of 4E-BP1 phosphorylation: a novel two-step mechanism. Genes Dev. *13*, 1422–1437. https://doi.org/10.1101/gad.13.11.1422.

39. Nishitoh, H. (2012). CHOP is a multifunctional transcription factor in the ER stress response. J. Biochem. *151*, 217–219. https://doi.org/10.1093/jb/mvr143.

40. Skardal, A., Devarasetty, M., Rodman, C., Atala, A., and Soker, S. (2015). Liver-Tumor Hybrid Organoids for Modeling Tumor Growth and Drug Response In Vitro. Ann. Biomed. Eng. *43*, 2361–2373. https://doi.org/10.1007/s10439-015-1298-3.

41. Shipley, L.A., Brown, T.J., Cornpropst, J.D., Hamilton, M., Daniels, W.D., and Culp, H.W. (1992). Metabolism and disposition of gemcitabine, and oncolytic deoxycytidine analog, in mice, rats, and dogs. Drug Metab. Dispos. *20*, 849–855.

42. He, J., Liu, D., Liu, M., Tang, R., and Zhang, D. (2022). Characterizing the role of SLC3A2 in the molecular landscape and immune microenvironment across human tumors. Front. Mol. Biosci. *9*, 961410. https://doi.org/10.3389/fmolb.2022.961410.

43. Liu, H., Deng, Z., Yu, B., Liu, H., Yang, Z., Zeng, A., and Fu, M. (2022). Identification of SLC3A2 as a Potential Therapeutic Target of Osteoarthritis Involved in Ferroptosis by Integrating Bioinformatics. Cells *11*, 3430. https://doi.org/10.3390/cells11213430.

44. Wang, H., Liu, C., Zhao, Y., Zhang, W., Xu, K., Li, D., Zhou, Y., Li, H., Xiao, G., Lu, B., and Gao, G. (2020). Inhibition of LONP1 protects against erastin-induced ferroptosis in Pancreatic ductal adenocarcinoma PANC1 cells. Biochem. Biophys. Res. Commun. *522*, 1063–1068. https://doi.org/10.1016/j.bbrc.2019.11.187.

45. Zheng, D.W., Lei, Q., Zhu, J.Y., Fan, J.X., Li, C.X., Li, C., Xu, Z., Cheng, S.X., and Zhang, X.Z. (2017). Switching Apoptosis to Ferroptosis: Metal-Organic Network for High-Efficiency Anticancer Therapy. Nano Lett. *17*, 284–291. https://doi.org/10.1021/acs.nanolett.6b04060.

46. Zong, W.X., Rabinowitz, J.D., and White, E. (2016). Mitochondria and Cancer. Mol. Cell. *61*, 667–676. https://doi.org/10.1016/j.molcel.2016.02.011.

47. Lavie, Y., Harel-Orbital, T., Gaffield, W., and Liscovitch, M. (2001). Inhibitory effect of steroidal alkaloids on drug transport and multidrug resistance in human cancer cells. Anticancer Res. *21*, 1189–1194.

48. Huang, Y., Li, G., Hong, C., Zheng, X., Yu, H., and Zhang, Y. (2021). Potential of Steroidal Alkaloids in Cancer: Perspective Insight Into Structure-Activity Relationships. Front. Oncol. *11*, 733369. https://doi.org/10.3389/fonc.2021.733369.

49. Diosa-Toro, M., Troost, B., van de Pol, D., Heberle, A.M., Urcuqui-Inchima, S., Thedieck, K., and Smit, J.M. (2019). Tomatidine, a novel antiviral compound towards dengue virus. Antivir. Res. *161*, 90–99. https://doi.org/10.1016/j.antiviral.2018.11.011.

50. Song, S.E., Shin, S.K., Cho, H.W., Im, S.S., Bae, J.H., Woo, S.M., Kwon, T.K., and Song, D.K. (2018). Tomatidine inhibits tumor necrosis factor-alpha-induced apoptosis in C2C12 myoblasts via ameliorating endoplasmic reticulum stress. Mol. Cell. Biochem. *444*, 17–25. https://doi.org/10.1007/s11010-017-3226-3.

51. Rodríguez-Martínez, J.A., Reinke, A.W., Bhimsaria, D., Keating, A.E., and Ansari, A.Z. (2017). Combinatorial bZIP dimers display complex DNA-binding specificity landscapes. Elife *6*, e19272. https://doi.org/10.7554/eLife.19272.

52. Axten, J.M., Romeril, S.P., Shu, A., Ralph, J., Medina, J.R., Feng, Y., Li, W.H.H., Grant, S.W., Heerding, D.A., Minthorn, E., et al. (2013). Discovery of GSK2656157: An Optimized PERK Inhibitor Selected for Preclinical Development. ACS Med. Chem. Lett. *4*, 964–968. https://doi.org/10.1021/ml400228e.

53. Yu, Q., Zhao, B., Gui, J., Katlinski, K.V., Brice, A., Gao, Y., Li, C., Kushner, J.A., Koumenis, C., Diehl, J.A., and Fuchs, S.Y. (2015). Type I interferons mediate pancreatic toxicities of PERK inhibition. Proc. Natl. Acad. Sci. USA *112*, 15420–15425. https://doi.org/10.1073/pnas.1516362112.

54. Skardal, A., Devarasetty, M., Forsythe, S., Atala, A., and Soker, S. (2016). A reductionist metastasis-on-a-chip platform for in vitro tumor progression modeling and drug screening. Biotechnol. Bioeng. *113*, 2020–2032. https://doi.org/10.1002/bit.25950.

55. Forsythe, S.D., Sivakumar, H., Erali, R.A., Wajih, N., Li, W., Shen, P., Levine, E.A., Miller, K.E., Skardal, A., and Votanopoulos, K.I. (2022). Patient-Specific Sarcoma Organoids for Personalized Translational Research: Unification of the Operating Room with Rare Cancer Research and Clinical Implications. Ann. Surg Oncol. *29*, 7354–7367. https://doi.org/10.1245/s10434-022-12086-y.

56. Martinez-Bosch, N., Vinaixa, J., and Navarro, P. (2018). Immune Evasion in Pancreatic Cancer: From Mechanisms to Therapy. Cancers *10*, 6. https://doi.org/10.3390/cancers10010006.

57. Thevenot, P.T., Sierra, R.A., Raber, P.L., Al-Khami, A.A., Trillo-Tinoco, J., Zarreii, P., Ochoa, A.C., Cui, Y., Del Valle, L., and Rodriguez, P.C. (2014). The stress-response sensor chop regulates the function and accumulation of myeloid-derived suppressor cells in tumors. Immunity *41*, 389–401. https://doi.org/10.1016/j.immuni.2014.08.015.

58. Cubillos-Ruiz, J.R., Bettigole, S.E., and Glimcher, L.H. (2017). Tumorigenic and Immunosuppressive Effects of Endoplasmic Reticulum Stress in Cancer. Cell *168*, 692–706. https://doi.org/10.1016/j.cell.2016.12.004.

59. Kim, Y.S., Yoon, J.W., Kim, D., Choi, S., Kim, H.K., Youm, J.B., Han, J., Heo, S.C., Hyun, S.A., Seo, J.W., et al. (2022). Tomatidine-stimulated maturation of human embryonic

stem cell-derived cardiomyocytes for modeling mitochondrial dysfunction. Exp. Mol. Med. *54*, 493–502. https://doi.org/10.1038/s12276-022-00746-8.

60. Lin, C.C., Ding, C.K.C., Sun, T., Wu, J., Chen, K.Y., Zhou, P., and Chi, J.T. (2021). The regulation of ferroptosis by MESH1 through the activation of the integrative stress response. Cell Death Dis. *12*, 727. https://doi.org/10.1038/s41419-021-04018-7.

61. Zhu, S., Zhang, Q., Sun, X., Zeh, H.J., 3rd, Lotze, M.T., Kang, R., and Tang, D. (2017). HSPA5 Regulates Ferroptotic Cell Death in Cancer Cells. Cancer Res. *77*, 2064–2077. https://doi.org/10.1158/0008-5472.CAN-16-1979.

62. Lánczky, A., and Győrffy, B. (2021). Web-Based Survival Analysis Tool Tailored for Medical Research (KMplot): Development and Implementation. J. Med. Internet Res. *23*, e27633. https://doi.org/10.2196/27633.

63. Mace, T.A., Shakya, R., Pitarresi, J.R., Swanson, B., McQuinn, C.W., Loftus, S., Nordquist, E., Cruz-Monserrate, Z., Yu, L., Young, G., et al. (2018). IL-6 and PD-L1 antibody blockade combination therapy reduces tumour progression in murine models of pancreatic cancer. Gut *67*, 320–332. https://doi.org/10.1136/gutjnl-2016-311585.

64. Gomez-Chou, S.B., Swidnicka-Siergiejko, A.K., Badi, N., Chavez-Tomar, M., Lesinski, G.B., Bekaii-Saab, T., Farren, M.R., Mace, T.A., Schmidt, C., Liu, Y., et al. (2017). Lipocalin-2 Promotes Pancreatic Ductal Adenocarcinoma by Regulating Inflammation in the Tumor Microenvironment. Cancer Res. *77*, 2647–2660. https://doi.org/10.1158/0008-5472.CAN-16-1986.

65. Kim, D., Langmead, B., and Salzberg, S.L. (2015). HISAT: a fast spliced aligner with low memory requirements. Nat. Methods *12*, 357–360. https://doi.org/10.1038/nmeth.3317.

66. Andrews, S. (2010). FastQC: A Quality Control Tool for High Throughput Sequence Data [Online]. http://www.bioinformatics.babraham.ac.uk/projects/fastqc/.

67. Liao, Y., Smyth, G.K., and Shi, W. (2014). featureCounts: an efficient general purpose program for assigning sequence reads to genomic features. Bioinformatics *30*, 923–930. https://doi.org/10.1093/bioinformatics/btt656.

68. Wang, L., Wang, S., and Li, W. (2012). RSeQC: quality control of RNA-seq experiments. Bioinformatics *28*, 2184–2185. https://doi.org/10.1093/bioinformatics/bts356.

69. Robinson, M.D., McCarthy, D.J., and Smyth, G.K. (2010). edgeR: a Bioconductor package for differential expression analysis of digital gene expression data. Bioinformatics *26*, 139–140. https://doi.org/10.1093/bioinformatics/btp616.

70. Gu, Z., Eils, R., and Schlesner, M. (2016). Complex heatmaps reveal patterns and correlations in multidimensional genomic data. Bioinformatics *32*, 2847–2849. https://doi.org/10.1093/bioinformatics/btw313.

71. Chen, J., Bardes, E.E., Aronow, B.J., and Jegga, A.G. (2009). ToppGene Suite for gene list enrichment analysis and candidate gene prioritization. Nucleic Acids Res. *37*, W305–W311. https://doi.org/10.1093/nar/gkp427.

72. Choueiry, F., Torok, M., Shakya, R., Agrawal, K., Deems, A., Benner, B., Hinton, A., Shaffer, J., Blaser, B.W., Noonan, A.M., et al. (2020). CD200 promotes immunosuppression in the pancreatic tumor microenvironment. J. Immunother. Cancer *8*, e000189. https://doi.org/10.1136/jitc-2019-000189.

73. Gadepalli, V.S., Ozer, H.G., Yilmaz, A.S., Pietrzak, M., and Webb, A. (2019). BISR-RNAseq: an efficient and scalable RNAseq analysis workflow with interactive report generation. BMC Bioinf. *20*, 670. https://doi.org/10.1186/s12859-019-3251-1.

74. Mascarenhas, R., Pietrzak, M., Smith, R.M., Webb, A., Wang, D., Papp, A.C., Pinsonneault, J.K., Seweryn, M., Rempala, G., and Sadee, W. (2015). Allele-Selective Transcriptome Recruitment to Polysomes Primed for Translation: Protein-Coding and Noncoding RNAs, and RNA Isoforms. PLoS One *10*, e0136798. https://doi.org/10.1371/journal.pone.0136798.

75. Strohecker, A.M., Guo, J.Y., Karsli-Uzunbas, G., Price, S.M., Chen, G.J., Mathew, R., McMahon, M., and White, E. (2013). Autophagy sustains mitochondrial glutamine metabolism and growth of BrafV600E-driven lung tumors. Cancer Discov. *3*, 1272–1285. https://doi.org/10.1158/2159-8290.CD-13-0397.

STAR★METHODS

KEY RESOURCES TABLE

REAGENT or RESOURCE	SOURCE	IDENTIFIER
Antibodies		
ATF-4 (D4B8) Rabbit mAb	Cell Signaling Technology	#11815; RRID: AB_2616025
4EBP1(53H11) Rabbit mAb	Cell Signaling Technology	#9644; RRID: AB_2097841
Phospho-4E-BP1 (Thr37/46) (236B4) Rabbit mAb	Cell Signaling Technology	#2855; RRID: AB_560835
CHOP (L63F7) Mouse mAb	Cell Signaling Technology	#2895; RRID: AB_2089254
GPX4 Antibody	Cell Signaling Technology	#52455; RRID: AB_2924984
F4/80 (D2S9R) XP® Rabbit mAb	Cell Signaling Technology	#70076; RRID: AB_2799771
CD8α (D4W2Z) XP® Rabbit mAb (Mouse Specific)	Cell Signaling Technology	#98941; RRID: AB_2756376
Rabbit monoclonal [Y92] to PDGFR alpha + PDGFR beta - C-terminal	ABCAM Inc	AB32570; RRID: AB_777165
Rabbit polyclonal to alpha smooth muscle Actin	ABCAM Inc	AB5694; RRID: AB_2223021
TROMA-III CK19	DSHB	AB2133570; RRID: AB_2133570
beta Actin Loading Control Monoclonal Antibody (BA3R)	ThermoFisher Scientific	MA5-15739; RRID: AB_10979409
β-Actin Antibody	Cell Signaling Technology	#4967; RRID: AB_330288
IRDye® 800CW Goat anti-Rabbit IgG (H + L), 0.5 mg	LiCOR Biosciences	926-32219; RRID: AB_1850025
IRDye® 680RD Goat anti-Mouse IgG Secondary Antibody 0.5 mg	LiCOR Biosciences	926-68070; RRID: AB_10956588
Goat anti-Rabbit IgG (H+L) Cross-Adsorbed Secondary Antibody, Alexa Fluor™ 488	ThermoFisher Scientific	A-11008; RRID: AB_143165
Chemicals, peptides, and recombinant proteins		
Tomatidine	MedChem Express	HY-N2149
Ferrostatin-1	MedChem Express	HY-100579
Cayman Chemical Erastin	Fisher Scientific	NC1511737
Gemcitabine	Selleck Chem	S1714
Hydroxypropyl-β-cyclodextrin	Sigma-Aldrich	332607-25G
DMSO	Sigma-Aldrich	D2650
ChIP Swelling Buffer	BIO WORLD	10450057-2
Photoinitiator	Advanced BioMatrix	5200
Neutralizing solution (for photo-collagen)	Advanced BioMatrix	5205
Thiolated HA	Glycosil, ESI-BIO	GS217
Methacrylated collagen type I	Advanced BioMatrix	5201
ProLong Gold Antifade Mountant	Life Technologies	P10144
ProLong™ Diamond Antifade Mountant	Life Technologies	P36970
Critical commercial assays		
MTT reagent	R&D Systems	4890-25-01
eBioscience Annexin V Apoptosis Detection Kit APC	Life Technologies	88-8007-72
RNeasy mini kit	QiaGEN	74104

(*Continued on next page*)

Continued

REAGENT or RESOURCE	SOURCE	IDENTIFIER
Opal Polaris 7 Color Manual IHC detection kit	Akoya Biosciences	NEL861001KT
ChIP-IT® Express Enzymatic	Active Motif	53009
Fast SYBRTM green master mix PCR kit	ThermoFisher Scientific	4385610
SuperScript™ III First-Strand Synthesis System	ThermoFisher Scientific	18080051
TaqMan Universal Master Mix II, no UNG	ThermoFisher Scientific	4440040
LIVE/DEAD viability/cytotoxicity kit for mammalian cells;	ThermoFisher Scientific	L3224
Promega CellTiter-Glo™ 3D Cell Viability Assay	Fisher Scientific	G9681
Invitrogen™ BODIPY™ 581/591 C11 (Lipid Peroxidation Sensor)	Fisher Scientific	D3861
Mito Stress Test kit	Agilent Technology	103010-100
Deposited data		
dbGaP data for scRNA seq analysis	Elyada et al.,[37]	phs002045.v1.p1
KM Plotter	Lanczky and Gyorffy,[62]	https://doi.org/10.1038/s41598-021-84787-5
Experimental models: Cell lines		
MiaPaca-2	ATCC	Cat#CRL1420; RRID: CVCL_0428
Panc1	ATCC	Cat#CRL1469; RRID: CVCL_0480
MT5	Mace et al.,[63]	KrasLSL−G12D, Trp53LSL−R270H, and Pdx1-cre mice
luciferase-tagged mouse KPC-luc cells	Gomez-Chou et al.,[64]	LSL-KrasG12D/+; TP53loxP/loxP; Pdx1-Cre mice
Experimental models: Organisms/strains		
C57BL/6 mice	The Jackson Laboratory	N/A
Oligonucleotides		
ChIP qPCR primer for heIF4EBP1	Integrated DNA Technologies (IDT)	(Seq1 CTCCTCCCCTCTCATTGT Seq2 CAGGATCTGTCGCGTTTTCT)
ChIP qPCR primer for CHOP (B site)	Integrated DNA Technologies (IDT)	(Seq1 GTGAGGGCTCTG GGAGGTGCT Seq2 AGGGGGATGTTACCTTTCCCTTCTC)
ChIP qPCR primer for ASNS	Integrated DNA Technologies (IDT)	(Seq1 CCTGTGCGCGCTGGTTGGTCCT Seq2 CGCTTATACCGACCTGGCTCCT)
Taqman Gene expression assay primers for ATF4	ThermoFisher Scientific	(Hs00909569_g1)
Taqman Gene expression assay primers for eIF4EBP1	ThermoFisher Scientific	(Hs00607050_m1)
Software and algorithms		
HISAT2 v2.1.0 (RRID:SCR_015530)	Kim et al.,[65]	http://ccb.jhu.edu/software/hisat2/index.shtml
FastQC (RRID:SCR_014583)	Andrews. S.,[66]	http://www.bioinformatics.babraham.ac.uk/projects/fastqc/
featureCounts (RRID:SCR_012919)	Liao et al.,[67]	http://bioinf.wehi.edu.au/featureCounts/
RSeQC (RRID:SCR_005275)	Wang et al.,[68]	http://code.google.com/p/rseqc/
edgeR (RRID:SCR_012802)	Robinson et al.,[69]	http://bioconductor.org/packages/edgeR/
Seahorse Wave (RRID:SCR_014526)	Agilent Technologies	http://www.agilent.com/en-us/products/cell-analysis-(seahorse)/software-download-for-wave-desktop

(*Continued on next page*)

Continued

REAGENT or RESOURCE	SOURCE	IDENTIFIER
ComplexHeatmap (RRID:SCR_017270)	Gu et al.[70]	https://bioconductor.org/packages/release/bioc/html/ComplexHeatmap.html
EnhancedVolcano (RRID:SCR_018931)	N/A	https://bioconductor.org/packages/EnhancedVolcano/
Ingenuity Pathway Analysis (IPA) (RRID:SCR_008653)	Qiagen	http://www.ingenuity.com/products/pathways_analysis.html
ToppGene (RRID:SCR_005726)	Chen et al.,[71]	http://toppgene.cchmc.org/
Prism 9 (RRID:SCR_002798)	GraphPad	http://www.graphpad.com/
SPSS Statistics version 28 (RRID:SCR_002865)	IBM	http://www-01.ibm.com/software/uk/analytics/spss/
Other		
Gibco™ DMEM, high glucose	Fisher Scientific	11-965-118
Gibco™ RPMI 1640 Medium, HEPES	Fisher Scientific	22-400-105
Fetal Bovine Serum, qualified, heat inactivated	Life Technologies	10438026
Antibiotic-Antimycotic (100X)	Life Technologies	15240062

RESOURCE AVAILABILITY

Lead contact

Further information and requests for resources and reagents should be directed to and will be fulfilled by the lead contact, Dr. Thomas A. Mace (Thomas.Mace@osumc.edu)

Materials availability

This study did not generate new unique reagents.

Data and code availability

- Data reported in this paper will be shared by the lead contact upon request. This paper also analyzes existing, publicly available data. These accession numbers for the datasets are listed in the key resources table.
- This paper does not report any original code.
- Any additional information required to reanalyze the data reported in this paper is available from the lead contact upon request.

EXPERIMENTAL MODEL AND STUDY PARTICIPANT DETAILS

Cells lines

Pancreatic cell lines MiaPaca-2 and Panc1 were cultured in DMEM (Gibco, Jenks, OK) with 10% FBS, 10 mM L-glutamine, and antibiotics. Murine MT5 (KrasLSL−G12D, Trp53LSL−R270H, and Pdx1-cre mice)[63,72] and luciferase-tagged mouse KPC-luc tumor cell line (derived from *LSL-KrasG12D/+; TP53loxP/loxP; Pdx1-Cre* mice)[64] were cultured in RPMI (Gibco) with 10% FBS, 10 mM L-glutamine, and antibiotics.

Animal studies

7-8 weeks old female C57BL/6 mice (n = 5/cage) used in this study. All animal protocols were approved by the Institutional Animal Care and Use Committee (IACUC) at The Ohio State University (Approved IACUC protocol 2009A0178-R3) and mice were treated in accordance with institutional guidelines for animal care. The Ohio State University Laboratory Animal Shared Resource is an Association for Assessment and Accreditation of Laboratory Animal Care International accredited program that follows Public Health Service policy and guidelines. All other experiments were completed under the research protocols (2014R00000086; 2013R00000056) approved by the Ohio State University Institutional Biosafety Committee.

METHOD DETAILS

Reagents

Tomatidine and Ferrostatin-1 were purchased from Med Chem Express (Monmouth Junction, NJ). Erastin was purchased from Cayman Chemicals (Ann Arbor, MI). Gemcitabine was purchased from Selleck Chemicals LLC (Houston, TX).

MTT viability assay

96-well plates were seeded at $2.5x10^3$ cells/well with human (Panc1, MiaPaca-2) and murine (MT5) pancreatic cancer cell lines and treated with increasing doses of tomatidine (0 μg/mL-12.8 μg/mL) and vehicle controls (DMSO). Post 72 hours of treatment, 10 μL of MTT reagent (R&D Systems; Minneapolis, MN) was added to the wells and incubated for 3 hours. Absorbance at 570 nm was read in the Epoch microplate spectrophotometer (BioTek; Winooski, VT). Percentage cell viability was evaluated relative to untreated control for each cell line.

Annexin V/PI staining

MiaPaca-2, Panc1, and MT5 cells were seeded at $2x10^5$ cells/well in a 6 well plate overnight and treated with increasing concentrations of tomatidine for 72 hours and assayed for cell death via apoptosis. Cell death was assessed by calculating cells positive for dual staining with annexin V and 7-AAD, which were performed using the eBioscience Annexin V Apoptosis Detection Kit APC (Life Technologies).

RNA sequencing

Total RNA was isolated using QiaGEN RNeasy mini kit according to the manufacturer's instructions. The purity of extracted RNA was measured using a NanoDrop ND-1000 spectrophotometer (NanoDrop Technologies LLC). The concentration was assessed by Qubit 2.0 Fluorometer (Agilent Technologies) using an RNA HS Assay Kit. Samples with RNA integrity number greater than 4 as assessed by a BioAnalyzer (Agilent Technologies) with no visible sign of genomic DNA contamination from the HS Nanochip tracings were used for total RNA library generation. The mRNA libraries were generated using the NEBNext® Ultra™ II Directional (stranded) RNA Library Prep Kit for Illumina (NEB #E7760L) using NEBNext Poly (A) mRNA Magnetic Isolation Module (NEB #E7490). NEBNext Multiplex Oligos for Illumina Unique Dual Index Primer Pairs (NEB #644OS/L) were used with a library input amount of 200ng total RNA (quantified using Qubit Fluorometer). Fragmentation was performed for 10 minutes with 12x amplification via PCR. Generated libraries were sequenced with Novaseq SP Paired-End 150bp format. The analysis of RNA-seq data was performed using custom-built bioinformatics workflow as described.[73] Briefly, quality-filtered raw reads were aligned to mouse reference genome GRCm38 or human reference genome GRCh38 using HISAT2 v2.1.0.[65] Quality control was conducted with fastqc, RSeQC, and picard.[66,68] Gene-wise counts were generated with featureCounts from the subread package v1.5.1 for genes annotated by ensemble GRCm38.102 for mouse or GRCh38.p13 for human reference genome.[67] Differentially expressed genes (DEGs) were determined using the R package edgeR[69] as described.[74] Genes with a false discovery rate (FDR) adjusted p value <0.05 and log2 fold change (log2FC) > 0.3 or < -0.3 were selected as differentially expressed genes and used for comparisons. Volcanos were plotted with R package EnhancedVolcano and heatmaps were plotted with R package ComplexHeatmap.[70]

Functional enrichment was performed with Qiagen Ingenuity Pathway Analysis (IPA) to enrich for IPA Canonical pathways and upstream regulator analysis. We used the ToppFun application of ToppGene[71] for the identification of enriched functional categories among DEGs. We also assessed enrichment of biological processes in gene ontology (GO) and Kyoto Encyclopedia of Genes and Genomes (KEGG) pathways. Bonferroni-corrected p values for the statistical tests of functional enrichment of less than 0.05 were considered statistically significant.

Kaplan-Meier (KM) plotter

To analyze the prognostic value of ATF4 in pancreatic cancer patients, Kaplan-Meier plotter was used. The publicly available Pan-Cancer RNA-Seq database with restrictions for grade III (n = 1510) patients with tumor type of PDAC (n = 177) were split into high and low ATF4 mRNA expression according to various quantile expressions. The two patient cohorts were compared by a Kaplan-Meier survival plot, and the hazard ratio with 95% confidence intervals and log rank p value were calculated. Databases and clinical data for KM Plotter are supervised and extended regularly.[62]

Multiplex immunofluorescence (IF)

FFPE slides were first incubated in a 60°C slide warmer for 1 hour. To completely remove paraffin, slides were placed in a glass slide rack and then immediately immersed in Xylene for 10 min thrice. Rehydration was achieved by sequentially immersing slides, for 10 min each, containing 100% ethanol, 90% ethanol and 70% ethanol followed by washing in deionized water for 2 mins. Following rehydration, slides were fixed using neutral buffered formalin for 30 minutes and washed with deionized water and TBS-T for 2 mins each. The slides were immersed in AR6 buffer (Akoya Biosciences) in a heat resistant box and microwaved at 20% power for 45s and consequently at 100% power for 15 min. After cooling to room temperature, slides were washed with deionized water and TBS-T followed by drying around the tissue and tracing the outside with a hydrophobic barrier pen. The slides were then placed in a humidified chamber and blocked using BLOXALL blocking solution for 10 mins followed by 1 hour of primary antibody incubation. This was followed with secondary antibody incubation and opal fluorophore incubation for 10 mins with intermittent washes with TBS-T thrice for 2 mins each. This cycle from microwaving to fluorophore incubation was repeated for the other primary antibodies in the panel. After the last round of staining, the tissue slides were incubated with spectral DAPI for 10 mins. After TBS-T washes, the slides were mounted using Diamond antifade mountant (ThermoFisher Scientific, Waltham, MA) and sealed using clear nail polish around the corners of the coverslip. The slides were then imaged using the Vectra Polaris and visualized using Phenochart.

ScRNA-seq dataset analysis

The dbGaP data (accession phs002045.v1.p1) was requested to access single cell RNA- sequencing of PDAC patients and stratified into cell populations based on gene expression profiles and clustering as reported in Table S1. ATF4 expression was assessed in different cell populations of the PDAC immune microenvironment.

Western blot

Tomatidine-treated cells were collected and lysed. Proteins were subjected to SDS-polyacrylamide gel (BioRad Mini Protean Tgx gradient gels; Hercules, CA) electrophoresis and then transferred to 0.45μm nitrocellulose membranes (BioRad) using Trans Blot-Turbo (BioRad). After blocking with Tris-buffered saline containing 0.5% BSA, membranes were incubated with each primary antibody in 0.5% BSA/TBS at 4°C overnight: ATF4, CHOP, p-4EBP1, 4EBP1, GPX4 (Cell signaling Technology; Danvers, MA), β-Actin loading control (InVitrogen; Waltham, MA). Membranes were then incubated with a IRDye-fluorescent anti-mouse or anti-rabbit secondary antibody (LiCOR Biosciences; Lincoln, NE) in 0.5% milk/TBS at room temperature for 1 h. Protein bands were visualized using LiCOR Odyssey CLx and analyzed via ImageStudio.

Immunofluorescence

4×10^4 Panc1 cells/well were plated on the NunC LabTek 4-chamber slides (ThermoFisher Scientific) and allowed to attach. The cells were treated with vehicle DMSO or 3.2 μg/mL tomatidine for 4 hours before being fixed in 4% formaldehyde at 37°C for 15 mins followed by permeabilization with 0.1% Triton-X for 10 minutes at room temperature. Overnight blocking and 1:75 primary antibody (ATF4) incubation was performed in 2% BSA and 0.1% BSA, respectively. 1-hour secondary antibody incubation was performed using 1:100 Alexa Fluor 488 followed by 10 minutes of DAPI incubation. Gold antifade mountant (ThermoFisher Scientific) was used for coverslipping and sealed with clear polish. For quantification, 10 different field of views were blindly assessed manually for expression of AF488 signal with respect to DAPI signal to evaluate nuclear vs. cytoplasmic translocation of ATF4. This was repeated for n = 3 biological replicates.

Chromatin immunoprecipitation and ChIP-qPCR

Chromatin immunoprecipitation was performed using Active Motif kit (Carlsbad, CA). Briefly, $2x10^7$ Panc1 cells were allowed to attach and were treated with tomatidine for 40 hours relative to untreated control. The cells were fixed with 1% formaldehyde for 10 minutes at room temperature (RT) and quenched via Glycine-stop-fix solution for 5 mins at RT. The cells were scraped using 1X PBS supplemented with 100 mM PMSF followed by incubation on ice with lysis buffer for 30 minutes. The cells were then exposed to hypertonic ChIP swelling buffer (BioWorld, Dublin, OH) supplemented with triton-X followed by 6 cycles of vigorous vortexing for 30s each followed by cold centrifugation to pellet the nuclei and digested using the digestion buffer for 5 minutes at 37 °C. The chromatin was enzymatically digested with 200U/ml of enzymatic shearing cocktail for 30 minutes at 37°C, vortexing every 2 minutes. The reaction was stopped using ice cold 0.5 M

EDTA followed by chilling on ice for 10 minutes and collecting the supernatant after centrifugation. Immunoprecipitation was set up using 20 μg of sheared chromatin with 5 μg of antiATF4 (Cell Signaling Technology) supplemented with 25 μl of pre-cleared Protein G magnetic beads overnight, protease inhibitor cocktail and ChIP Buffer 1 at 4°C overnight on an end-to-end rotor and at 4°C. Beads were washed sequentially by ChIP buffer 1 and 2 and eluted using 50 μL of AM2 Elution buffer for 15 min at RT. This was followed by 50 μL of reverse cross-linking buffer at 65°C for 2.5 hours. The tubes were incubated with Proteinase K for 1 hour at 37°C. DNA was subjected to a clean-up using Active Motif Chromatin IP DNA Purification Kit. RT-qPCR was performed using specific primers for heIF4EBP1 (Seq1 CTCCTCCCCTCTCATTGT Seq2 CAGGATCTGTCGCGTTTTCT), CHOP (Seq1 GTG AGG GCT CTG GGA GGT GCT Seq2 AGG GGG ATG TTA CCTTTCCCTTCTC) and ASNS (Seq1 CCTGTGCGCGCTGGTTGGTCCT Seq2 CGCTTATACC GACCTGGCTCCT). Input DNA and Negative control IgG Antibody was used as a control to assess the differences in ATF4 binding between untreated and tomatidine treated samples with Fast SYBR™ green master mix (ThermoFisher Scientific) PCR kit.

In vivo experiments

7-8 weeks old female C57BL/6 mice (n = 5/group) were injected with 1 × 10^6 MT5 cells subcutaneously. 4g hydroxypropyl-β-cyclodextrin was dissolved in 6 mL sterile water to prepare 40% hydroxypropyl-β-cyclodextrin (HPBCD). 40% HPBCD was used to dissolve tomatidine for the purpose of intraperitoneal injection. When the tumors were palpable (~50 mm3), the mice were treated intraperitoneally with vehicle control (40% HPBCD) or 5 mg/kg Tomatidine once a day. Tumor volumes were measured until vehicles reached early removal criteria and study endpoint. Tumors were collected in RNALater (Thermo Fisher Scientific, Waltham, MA) and processed for RNA isolation at study endpoint. 7–8 weeks old female C57BL/6 mice (n = 5/group) were injected with 2.5x10^5 KPC-Luc cells orthotopically.[63] The tumors were visualized via luminescence IVIS imaging and randomized, before starting treatment. The mice were divided into four groups and treated intraperitoneally. Treatment groups were vehicle (40% hydroxypropyl-β-cyclodextrin) or 5 mg/kg single agent Tomatidine once per day or 10 mg/kg single agent gemcitabine twice a week or combination of both tomatidine and gemcitabine regimen. Tumor weights were measured at study endpoint.

qRT-PCR

Tumors (<30 mg) saved in RNALater were processed to isolate RNA by Qiagen RNeasy Mini Prep RNA isolation kit. 1000 ng of RNA was used to make cDNA bySuperScript™ III First-Strand Synthesis System (ThermoFisher Scientific). The cDNA was evaluated for ATF4 and eIF4EBP1 mRNA expression using TaqMan Universal Master Mix II, no UNG (Life Technologies, Carlsbad, CA) and Taqman Gene expression assay primers for ATF4 (Hs00909569_g1), and eIF4EBP1 (Hs00607050_m1).

Organoid formation

ECM-mimicking Collagen-Hyaluronic acid (HA) hydrogels were formed using HyStem-HP (ESI-BIO, Alameda, CA). The thiolated HA (Glycosil, ESI-BIO) component was dissolved in water containing 0.1% w/v of the photoinitiator 4-(2- hydroxyethoxy) phenyl-(2-propyl) ketone to make 1% w/v solutions. 52μL of methacrylated collagen type I (Advanced BioMatrix, San Diego, CA) was added to 18.75 μL of the HA and 4.41 μL of neutralizing solution (for photo-collagen) in a small conical tube. Cells were added to this resulting solution and 5 μL organoids were constructed for each well of a 48-well plate previously coated with a thin layer of polydimethylsiloxane (PDMS). Organoids were photopolymerized in place using a brief UV light pulse (365 nm, 18 W cm^{-2} for 2s) to initiate crosslinking of the hydrogel. The organoids were then treated with 7 μg/mL and 28 μg/mL of Tomatidine, 3μM Gemcitabine, a combinational dose of the 28 μg/mL of Tomatidine and 3 μM Gemcitabine; 0 μM dose is used as control/vehicle.

Phenotypic and functional assays for 3D ECM-mimicking Collagen-Hyaluronic acid (HA) hydrogels

LIVE/DEAD staining (LIVE/DEAD viability/cytotoxicity kit for mammalian cells; Thermo Fisher, Waltham, MA) was performed 24 and 72 hours post drug exposure. Spent medium was first aspirated from wells, after which 250 μL of mixture of PBS and DMEM (1:1) containing 0.5 μM calcein-AM and 2 μM ethidium homodimer-1 was introduced to each well. Organoids were incubated for 30 minutes, after which fluorescent imaging was performed using a Nikon A1R confocal microscope. z-Stacks (200 μm) were obtained for each construct using filters appropriate for both red and green then superimposed. Viability was also

assessed via luminescence using Cell Titer-Glo 3D cell viability assay. Spent media was aspirated from wells and a 1:1 mixture of 3D ATP media and DMEM was added. The well-plate was gently shaken for 5 minutes and then incubated at room temperature for 25 minutes. Luminescence was measured on a microplate reader (Varioskan LUX 3020-80022).

C11 bodipy assay

1.25×10^5 Panc1 and MiaPaca-2 cells were plated on 6 well plates and allowed to attach for 24 hours. After 16 hours of treatment with 6.4 μg/mL tomatidine and 5 μM Erastin with and without 5 μM Ferrostatin-1 (Fer-1), cells were incubated with C11 Bodipy (1mg/ml) for 20 min. Cells were collected, washed, and resuspended in 500 μL PBS. They were then assessed for FITC positivity using flow cytometry.

Seahorse assay

Mitochondrial energetics were profiled in Panc1 cells with the Seahorse Biosciences extracellular flux analyzer (XFe24) as described previously.[75] Panc1 cells were seeded at 2×10^4 cells per well in XFe24 plates in 150 μL of DMEM (10% FBS, 1% Pen-Strep) and allowed to attach for an hour in a standard cell culture incubator (37°C and 5% CO_2). Once adhered, 350 μL of additional growth medium was added to each well, bringing the total volume to 500 μL. The cells were then allowed to grow overnight in a standard cell culture prior to XF assay. Cells were treated with the indicated concentrations of Tomatidine or DMSO vehicle for 6h at 37°C. Following treatment, cells were washed twice with PBS and incubated with 500 μL of freshly prepared DMEM XF Base media pH 7.4 (Agilent 103575-100) supplemented with 10mM glucose, 1mM sodium pyruvate, and 2mM L-glutamine, transferred to a 37°C non-CO_2 incubator and de-gassed for one hour prior to analysis with the Mito Stress Test kit (Agilent, 103010-100) run according to manufacturer's instructions (1.5 μM oligomycin, 1 μM FCCP, and 0.5 μM each of rotenone and antimycin). Data was normalized to cell count.

QUANTIFICATION AND STATISTICAL ANALYSIS

Data are presented as the means ± standard error of the mean (SEM) unless stated otherwise. All *in vitro* experiments consisted of three or more biological replicates per experimental group. *In vivo* studies consisted of five mice per group. No data were excluded from the statistical analyses. For comparisons between two groups, a two-tailed independent samples t-test was applied. For comparisons among three or more groups, one-way ANOVA with Tukey's post-hoc test was applied, as indicated. A p value <0.05 was deemed as the significance threshold for all analyses. p values were calculated as mentioned above, and *, **, and *** are used to denoted $p < 0.05$, $p < 0.01$, and $p < 0.001$, respectively, in figures and tables. Analyses were performed using Prism 9 (GraphPad (RRID:SCR_002798)) software and verified via IBM SPSS (RRID:SCR_002865) Statistics version 28.